Theoretical Models for Sputtering and Desorption of Bio-Organic Molecules under Collisional and Electronic Excitation by Ion Impact

By C.T. Reimann

Division of Ion Physics, Department of Radiation Sciences

Uppsala University, Box 535, S-751 21 Uppsala, Sweden

Synopsis

Particle-beam excitation of materials composed of thermally labile bio-organic molecules causes sputtering into the gas phase of intact molecules as well as their fragments. The desorbed ionic components, easily detected, form the basis for mass spectrometric applications. Keen interest in understanding desorption phenomena has been driven by the prospects for measuring increasingly higher molecular masses. The key question is: How can a fragile bio-organic molecule be desorbed intact by an inherently destructive incident energetic ion? In this paper, several prominent desorption theories are reviewed. Models involving 'collective' motion, such as the 'pressure pulse' model, seem most effective at explaining how large molecules acquire enough momentum to be desorbed without simultaneously acquiring enough internal energy to be dissociated. Weaknesses in the current state of our knowledge are identified. In particular, a lack of comprehensive knowledge on ejection of neutral molecules strongly impedes the validation of theoretical models.

Contents

1 Introduction

It is well known that sputtering of bio-molecular ions may be induced by energetic particle impacts on organic targets. Reports on MeV-fission-fragment-induced desorption were first published by Torgerson et al. (1974) and Macfarlane & Torgerson (1976). Meanwhile, Benninghoven et al. (1976) observed that keV atomic ions can also induce desorption of biomolecular ions. Finally, scattered works have appeared on keV cluster- and molecular-ion-induced desorption of molecules from organic targets. Recent examples include the works of Ledbetter et al. (1987), Mahoney et al. (1991), Kaufmann et al. (1992), and Martens et al. (1992).

In a generic ion impact desorption experiment, energetic projectiles impinge on an organic solid composed of bio-molecules which are bound together by hydrogen, ion-pair, and van der Waals bonds. A typical cohesive binding energy is of the order of a few electron volts (eV) per molecule. Close to the projectile path through the solid, the deposited energy density is extremely high and causes extensive fragmentation of target molecules. But over time, locally deposited energy diffuses outwards from the initially excited region. Eventually, several different kinds of species are desorbed from the target, including neutral and charged fragments and whole molecules. The observation of intact bio-molecule ejection has proved particularly interesting in view of the inherently damaging nature of the incident energetic projectiles. The readily detected desorbed ions form the basis of powerful mass spectrometric techniques applicable in the biological sciences.

A desorption event in response to an energetic projectile impact is the end result of a large number of processes, all of which are in principle amenable to theoretical treatment. One would begin by modelling energy deposition and the creation of kinetic energy in the excited solid. In the case of keV atomic and cluster projectile impact, target particle motion is directly excited, but in the case of MeV atomic projectiles, target particles are set in motion indirectly through relaxation of electronically deposited energy. This conversion occurs via relaxation of repulsive electronic states (as in the case of a Coulomb explosion, for example), molecular expansion after vibrational excitation, or chemical energy release. One would next model what could be referred to as 'direct' desorption processes in

which a particular molecule is ejected due to its own repulsive interactions with neighbouring molecules. One would then proceed to model what could be referred to as 'indirect' desorption processes which reflect the spatial evolution of energy to regions quite far beyond that in which energy is initially deposited. Finally, one would model the further evolution that may take place in energized species during and after desorption. Such further evolution may modulate the charge state and degree of clustering or fragmentation, determining critically what species is eventually detected far away from the sample.

A brief consideration of salient experimental results provides strong indications that indirect desorption mechanisms are of dominant importance for desorption of organic materials under particle beam excitation. Consider first the case of MeV atomic ions incident on organic solids. A typical example is 90 MeV $^{127}I^{14+}$ incident on a leucine target (MW 131 u). The electronic stopping power $(dE/dx)_e$ of the ions in this target is about 1000 eV/Å; approximately half of the ion energy is deposited within an 'infratrack' of radius 5.6 Å (Brandt & Ritchie, 1974), giving an energy density there of about 5.1 eV/Å^3. The volume occupied per leucine molecule is approximately 125 Å^3, meaning that each leucine molecule in the infratrack receives 640 eV of energy. Since the total internal molecular binding energy of leucine is only about 100 eV, molecules in the infratrack will be completely fragmented. Because energetic secondary electrons leave the infratrack and cause additional modifications to surrounding target material, the radius 5.6 Å can be considered to be a lower limit on the size of the region which is completely damaged by the incident ion. Salehpour et al. (1986) have examined the fluence dependence of the desorbed leucine ion signal, which they have used to extract 'damage radii' of around 30 Å. Because the ion yield may not be representative of the much larger neutral yield, the interpretation of the ion fluence dependence in terms of damage is tentative, and 30 Å should be regarded as a rough upper limit on the size of the region which is completely damaged by the incident ion. Salehpour et al. (1986) have also measured the neutral ejection yield of leucine molecules to be about 1200 leucine molecules per incident ion. If the desorbed volume is assumed to be a half-sphere, then the radius of this volume is around 40 Å, larger than the above estimates of the damaged area around the ion track and much larger than the size of the primary excited region of the ion track. Thus, a large number of ejected intact molecules come from outside the region of the target which is directly excited and damaged by the incident energetic particle.

Consider next the case of keV atomic projectiles incident on an organic material. Such ions slow down mainly by undergoing screened elastic nuclear collisions which set target atoms in motion. (A small fraction of the projectile energy is lost in ionization events as well.) Whitlow et al. (1987) have performed computer simulation studies of the slowing down of 10 keV Xe ions in a biomolecular target

(relative atomic composition: C_3H_5NO, 71 u). In these simulations, although the range of this projectile into the target is 200 Å, at a distance of only 10 Å laterally away from the ion track the deposited energy density is already an order of magnitude less than it is at the impact point. Wong et al. (1985) measured the absolute sputtering yield of 6 keV Xe ions incident on liquid glycerol (92.09 u) and found it to be in excess of 1000 glycerol molecules per incident ion. If the desorbed material is assumed to come from a contiguous volume in the form of a half-sphere, then the diameter of this volume is at least 80 Å, quite a bit larger than the apparent radial extent of the collision cascade. Even the assumption that the whole energized region of the target is ejected as a gas jet would only account for about half of the observed ejection yield. Again, one concludes that a large number of ejected intact molecules come from outside the region of the target which is directly excited by the incident energetic particle.

Finally, consider the case of keV and MeV clusters impacting organic targets. Ledbetter et al. (1987) have bombarded tobacco mosaic virus with energetic water clusters such as 275 keV $(H_2O)_{200}H^+$. The impact of such an ion on this organic target generally removed a 160 Å long 'slice' of the 180 Å diameter cylindrical virus, the slice being perpendicular to the long cylindrical axis. The water cluster ions employed in the virus bombardment study are thought to be 'ice balls' rather than 'snow flakes', meaning that their diameters range from 23 to 50 Å depending on their exact shape. Each oxygen atom in the projectile has a kinetic energy of about 1.2 keV, and neglecting cluster effects, such an atom would deposit its energy in a volume of diameter 30 to 40 Å based on simple stopping power considerations and a primitive collision cascade picture. Comparing the volume of the initially energized region of the virus to the volume of the impact-induced crater, it is seen that 90 to 95% of the desorbed molecules come from outside the initially energized region.

Johnson (1987) performed an extensive review of theoretical models extant at that time, and Sundqvist (1991) and Johnson & Sundqvist (1992) have given short summaries of the current experimental and theoretical status of biomolecular desorption. However, there does not seem to exist any extensive and comprehensive current review of theories of particle impact induced organic molecule desorption. In this article, such a review is attempted. The main theories which are covered are: collision cascade; ion track; evaporative thermal spike; bulk desorption (gas-flow); shock wave; and pressure pulse. In each case, the theory is described in some detail, and its validity in various arenas of applicability is specified. Because currently available experimental evidence suggests that ejected molecules come from relatively far away from the region that is initially energized, it is concluded that ejection mechanisms characterized by 'indirectness' or 'collective motion imparted at a distance' are currently the most satisfactory. Consequently, bulk desorption,

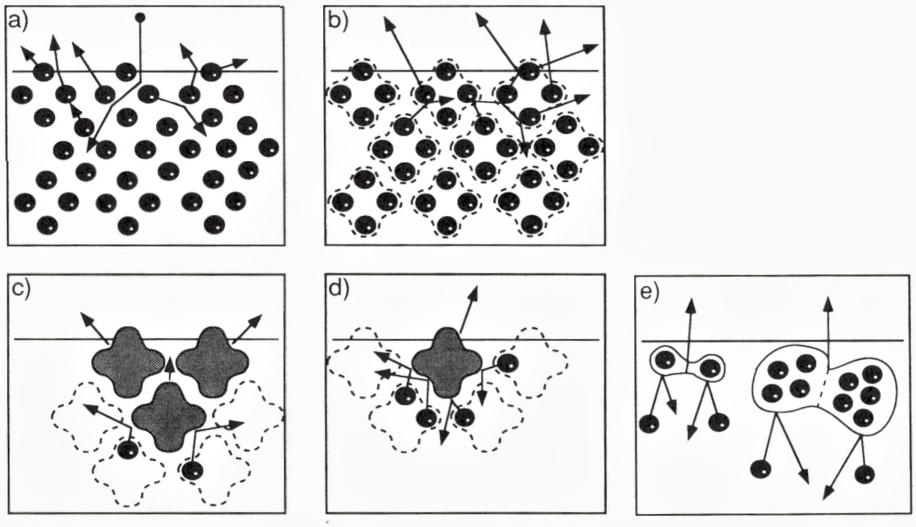

Figure 1. Schematic diagrams of collision cascade sputtering of atoms and molecules. a) Collision cascade in an atomic solid. Five atoms are sputtered. b)-d) Collision cascades in an organic solid. b) At early times, the cascade has an atomic character. c) At late times, the cascade has a molecular character. d) One molecule being ejected by several atoms impacting from below. e) Schematic diagram of statistical models. Left, model of Haring et al. (1987). Right, model of Hoogerbrugge & Kistemaker (1987).

shock waves, and pressure pulses describe the widest range of data, though other models discussed are not without their regimes of applicability. Molecular dynamics simulation results are included as theory and are discussed where applicable, and it is seen that well-designed simulations provide crucial insight into both experimental and analytical theoretical results. It is finally noted that the lack of comprehensive data on ejection of neutral bio-organic molecules is a strong impediment to evaluating the validity of theoretical models. Therefore, experimentalists are directed to devote more effort to probing the neutral ejecta.

2 Collision-Cascade Desorption

The collision cascade model is considered to be germane mainly for cases in which keV atomic ions are incident on solid matter. In this 'low velocity' regime, the projectile velocity v_0 is less than the Bohr velocity v_{Bohr}, and the incident ion energizes atoms in the target through screened elastic nuclear collisions. Target atoms, set into motion, undergo subsequent collisions, setting a second generation

of atoms into motion. The total ensemble of energized atoms is referred to as a 'collision cascade' as long as the energy density is not 'too high'. The energy density is considered to be too high if most of the atoms in the collisionally energized region of the target are in motion, or if moving atoms tend to collide with other moving atoms rather than with atoms at rest. A schematic diagram of an atomic collision cascade is shown in fig. 1a.

Collision cascade theory for atomic solids is well-established and has been described at length by Sigmund (1969, 1969a, 1981). A Boltzmann integral equation approach is employed with its underlying assumption of 'molecular chaos' and randomization of the particle coordinates and velocities after each collision according to some statistical distribution function. Solution of the Boltzmann integral equation leads to the conclusion that, inside the solid, the distribution of recoil atoms is isotropic and is characterized by a kinetic energy spectrum $N(E) \propto E^{-2}$. This is the result of a series of two-body collisions between moving and stationary atoms. Taking into account energy lost by atoms moving towards the surface and the surface barrier, total and differential sputtering yields are calculated. For rather low incident particle kinetic energies and high desorbed atom kinetic energies, the desorbed atom kinetic energy spectrum scales as E^{-2}. The peak in the energy distribution is located at $U/2$, where U is the surface binding energy. The sputtering yield is proportional to the nuclear stopping power, $(dE/dx)_{\mathrm{n}}$. This model describes quite well the sputtering of metal targets by keV atomic ions. Falcone (1987, 1990) has presented additional comments on collision cascade theory.

The question of how collision cascade theory should be generalized to the case of a molecular solid is in detail a complex one. Hoogerbrugge and Kistemaker (1987) have pointed out that the initial, more energetic portion of the collision cascade can be described by the atomic collision cascade model, but that 'in a later, low energy, stage of the cascade the presence of relatively strong bonds forces the complete molecules to take part in the collisions and the atomic picture loses its value.' Schematic diagrams showing the situations at these extremes in time are shown in fig. 1b,c. One theoretical approach to collision cascade sputtering of molecules is a 'statistical' model in which a point of view intermediate to the atomic and molecular pictures is taken. In this model, a molecule at the surface is assumed to be impacted from below by a number of atoms, and these impacting atoms are assumed to have a kinetic energy distribution given by the atomic collision cascade picture, $N(E) \propto E^{-2}$. This simplified situation is shown in fig. 1d.

Haring et al. (1987) have calculated kinetic energy and angular distributions of desorbed diatomic molecules using the statistical model, and they have generalized their results to the cases of larger polyatomic molecules. Their model is based closely on a similar model due to Können et al. (1975), which describes the desorption of clusters formed from separate atoms on the surface. Briefly, each

atom ('target atom') in the polyatomic molecule to be desorbed is assumed to be impacted by a moving atom from the substrate below. The target atom is assumed to gain kinetic energy as though it were a participant in a collision cascade; that is, after the collision, it is characterized by an isotropic velocity distribution and kinetic energy spectrum $N(E) \propto E^{-2}$. The momenta acquired by the target atoms are assumed to be uncorrelated. The resulting distribution in total momentum and internal energy is given as an integral over a product of the single atom momentum distribution functions $\chi(p)$ with the proviso that the total internal energy must not exceed the binding energy of the molecule. The final desorbed molecule parameters are calculated as in standard collision cascade theory. The chief result of this theory is as follows: for a polyatomic molecule consisting of m atoms, each of which is impacted by one recoil atom from a collision cascade in the substrate, the desorbed molecule kinetic energy spectrum for large kinetic energies scales as $E^{0.5-2.5m}$. For $m = 1$, the kinetic energy distribution for high kinetic energies reduces to the usual form, which is proportional to E^{-2} for the atomic collision cascade. The steeper energy distribution for polyatomics is related to the possibility for fragmentation if the internal energy is too great. Urbassek (1987) has made additional comments on the sputtering of molecules by a collision cascade.

Hoogerbrugge & Kistemaker (1987) have extended the model of Haring et al. (1987) in the sense that a polyatomic molecule containing $m > 2$ atoms is considered to be impacted by exactly two atoms originating in a collision cascade. Each atom from below is assumed to collide with a portion, or 'sub-unit', of the molecule to be desorbed. A schematic diagram of the proposed idea is shown in fig. 1e. Each sub-unit is considered to receive a correlated momentum as a whole, but the momenta of the two sub-units are assumed to be uncorrelated. For a molecule composed of two sub-units, momentum space analysis yields an asymptotic kinetic energy spectrum which is the same as that predicted by Haring et al. (1987) for a diatomic molecule impacted by two collision cascade atoms. That is, the desorbed molecule kinetic energy distribution is proportional to $E^{-4.5}$ for high kinetic energies.

Garrison (1983) has employed a classical dynamics simulation to demonstrate that collision cascade sputtering of organic molecules is indeed feasible. The simulated situation was that of a 1 keV Ar^+ incident upon a Ni(001) crystal on the surface of which had been adsorbed flat organic molecules as large as $C_{24}H_{12}$ (300.4 u). The simulation results suggest that a cascade in the underlying solid is capable of ejecting large organic admolecules from the surface. However, such admolecules have to be struck simultaneously by two or three atoms from the underlying solid in order for ejection of the intact molecule to take place. This is a good example of what appears to be a general principle: desorption of a large molecular moiety with sufficiently low internal energy to avoid fragmentation requires some kind of

'collective' desorption process, in this case a fortuitous push in the same general direction by several atoms colliding from below.

Well-designed classical dynamics simulations may be employed in order to gain an intuitive feel for the validity of statistical models in describing molecular desorption during collision cascades. Shapiro & Tombrello (1992) have reported results of classical dynamics studies of ejection of dimers and larger clusters from ion bombarded Cu. Those authors judge that statistical models even of dimer ejection are too simplistic to adequately describe the cluster ejection process. In particular, the surface is not well-defined when cluster ejection occurs, and each atom in the cluster undergoes multiple (and probably correlated) collisions with various underlying and neighbouring atoms. The possible parallels between cluster desorption and molecule desorption, exploited to generate the statistical models discussed above, are obvious but have not yet been validated extensively. Probably classical dynamics simulations are an important key to understanding collision cascade desorption of molecules from surfaces.

In the general arena of bio-organic molecule desorption, collision cascade theory has mostly been applied to the case of sputtering of molecular ions from glycerol, a commonly employed fast atom bombardment (FAB) matrix. Typically, no consideration is given to the fact that one detects desorbed ions but compares the measurements with results of theories of neutral particle ejection. One focus of experimental work has been on measuring the desorbed ion kinetic energy distribution in the limit of large kinetic energies. Generally, asymptotic power laws of the form E^{-x} are observed. A good example of this work is that of Hoogerbrugge et al. (1987) who have studied the emission of ions like Na^+, $GlyNa^+$, and $(NaCl)_2Na^+$ from a glycerol matrix. The theoretical results of Haring et al. (1987) and Hoogerbrugge & Kistemaker (1987) were generalized to obtain the number of 'hits' necessary to desorb an ion: $m = (x + 0.5)/2.5$. For the ions listed above, m = 1.0, 2.1, and 3.3 were respectively obtained. In general, m was rather close to being an integer, supporting its interpretation as a number of 'hits'. Since some of the molecular ions contained more than three atoms, a 'hit' is considered to involve a group or 'sub-unit' of atoms in the molecule.

Even though collision cascade desorption probably does occur for these glycerol liquid matrices, the model does not account for the dominant fraction of the yield. Yen et al. (1992) and Yen (1992) have studied the ion yield from pre-formed analyte molecular ions bound to the surface of a glycerol liquid drop by a surfactant. The ion sputtering yield scales as $[(dE/dx)_n - C]^2$, where $(dE/dx)_n$ is the nuclear stopping power and C is a threshold parameter. By contrast, the collision cascade model predicts linear scaling in $(dE/dx)_n$. Also, Kelner & Markey (1984) show clear evidence that the peak in the kinetic energy spectrum of desorbed poly (ethyleneglycol) ions (133 u) varies by more than a factor of two as the Ar^+ projectile

energy varies from 2 to 4 keV, also at odds with the predictions of the collision cascade model. It is widely suspected that low energy desorbed molecular ions from keV ion-bombarded glycerol are produced by a thermal 'bulk desorption' type mechanism or a pressure pulse, and that only the high energy sputtered particles reflect a collision cascade that occurs early on before the surface is catastrophically disrupted. The ideas of bulk desorption and pressure pulses are discussed below.

Studies have been performed by Standing et al. (1982) and Ens (1992) on bombardment of solid organic samples by 1 to 16 keV primary alkali ions. For the heavier alkali ions, Na^+, K^+, and Cs^+, ion sputtering yields scale as $(dE/dx)_n^3$, which is at variance with the predictions of simple collision cascade theory. For the relatively light Li^+ projectile, the electronic energy loss also plays a role, since $(dE/dx)_e$ and $(dE/dx)_n$ are comparable. Even so, the sputtering yield in this case scales as a linear combination of $(dE/dx)_n^3$ and $(dE/dx)_e^2$. For solid organic targets, it also seems that collision cascades do not play a dominant role in the ejection of bio-organic molecules.

3 Hit Theory Description of Desorption

The 'hit theory' approach to organic molecule desorption is designed for cases in which incident MeV atomic ions are responsible for the initial excitation. Such ions deposit energy electronically according to the electronic stopping power, $(dE/dx)_e$. About half of the deposited energy appears in a cylindrical 'infratrack' of radius of the order of 5 Å, and the other half of the deposited energy appears in a cylindrical 'ultratrack', which is of considerably larger radius. The chief means of depositing energy in the ultratrack is by energetic secondary electrons ('delta rays'), which emanate from the infratrack and create additional electronic excitation and ionization events in the surrounding material. The central idea of hit theory is that if a molecule near the surface receives at least i_{min} hits, i.e. if at least i_{min} secondary electrons interact with it, then the molecule is desorbed, possibly as an ion. Hit theory has been employed to account for the observed $(dE/dx)_e$ dependence of the ion desorption yield. The general idea of hit theory was introduced by Katz (1968). The application of hit theory to desorption, giving the ion track model, was introduced by Hedin et al. (1985) and has been recapitulated by Johnson (1987).

A schematic diagram of an organic molecule bound to a surface is shown in fig. 2. Both inter- and intra-molecular bonds are shown. The molecule is assumed to be bathed in a flux of secondary electrons due to the nearby passage of an MeV atomic ion through the material. The desorption of the intact molecule under these conditions requires the preservation of all internal bonds and the breaking (excitation to an anti-bonding state) of some of the external bonds. The charge of the

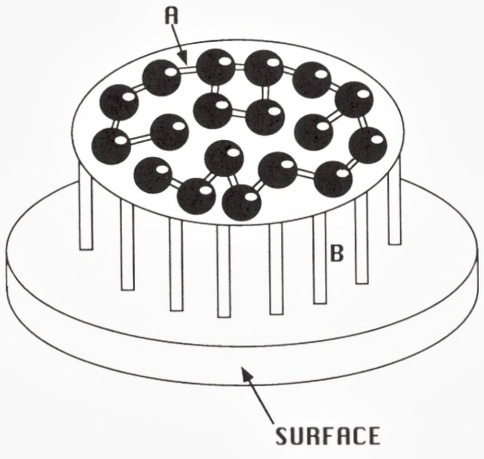

Figure 2. Schematic diagram of an organic molecule showing both internal bonds (A) and bonds to surrounding molecules in the surface (B). Successful desorption requires breaking all the bonds B while leaving all bonds A intact. Ionization will require some additional bonding adjustments.

desorbed species, if not predetermined, depends on some additional adjustments in bonding. Hit theory is basically a statistical description of these bonding modifications. In deriving the hit theory desorption model, the average number of hits experienced by a molecule must be calculated. Let $\eta_{\mathrm{F}}(r)$ be the average number of internal bonds broken in a molecule located a perpendicular distance r from the incident ion track. Correspondingly, $\eta_{\mathrm{D}}(r)$ will be the average number of external bonds broken. One may write:

$$\eta_{\mathrm{F}}(r) = \frac{\varepsilon(r)}{n_{\mathrm{M}} W_{\mathrm{F}}};\ \eta_{\mathrm{D}}(r) = \frac{\varepsilon(r)}{n_{\mathrm{M}} W_{\mathrm{D}}} \tag{1}$$

where $\varepsilon(r)$ is the energy density deposited by secondary electrons at a distance r from the ion track, n_{M} is the molecular number density, and W is a bond breaking energy. The nature of $\varepsilon(r)$ was discussed by Hedin et al. (1985). They pointed out that the detailed nature of secondary electron energy loss and the kinetic energy distribution of the secondary electrons give rise to a simple approximation for $\varepsilon(r)$:

$$\varepsilon(r) \propto \frac{(dE/dx)_{\mathrm{e}}}{r^2}. \tag{2}$$

Next a key assumption is made: The number of hits experienced by a molecule is described by the Poisson distribution. Then, if the average number of hits is η, the

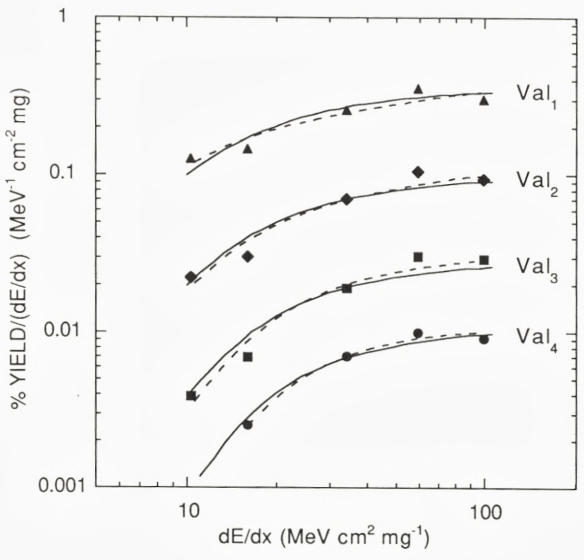

Figure 3. Ion sputtering yield divided by electronic stopping power $(dE/dx)_e$ vs. $(dE/dx)_e$ for valine monomers and clusters from MeV-heavy-atomic-ion-excited valine. For experimental details, see Hedin et al. (1985). The solid lines represent the results of the ion track model of Hedin et al. (1985). In the order from monomer to tetramer, the number of hits required to fit the data is 4, 5, 6 and 7 respectively. The dashed lines represent the results of an evaporative thermal model by Lucchese (1987). Both of these models are discussed in the text.

probability of a molecule experiencing exactly i hits is:

$$\Pr(i) = \frac{\eta^i}{i!} e^{-\eta} \tag{3}$$

An expression for the desorption yield of molecular ions can then be written. It assumes that only molecules receiving no damage hits are desorbed intact, and that desorption requires at least $i_{\min}$ hits of the desorptive type. Two details are specified as proportionality constants: the probability that the molecule is desorbed as an ion is P_{ion}, and the average depth from which ion desorption occurs is Z_{avg}. The desorption yield is then given as an integral over the surface of the sample with the ion track located at the center:

$$Y = P_{\text{ion}} Z_{\text{avg}} n_{\text{M}} \int_{r_{\text{d}}^2}^{\infty} \pi d(r^2) e^{-\eta_{\text{F}}(r)} \sum_{i=i_{\min}}^{\infty} \frac{\eta_{\text{D}}^i(r)}{i!} e^{-\eta_{\text{D}}(r)}. \tag{4}$$

The lower integration limit, r_{d}, takes into account that a direct collision between the incident ion and the target molecule causes complete fragmentation; r_{d} is roughly

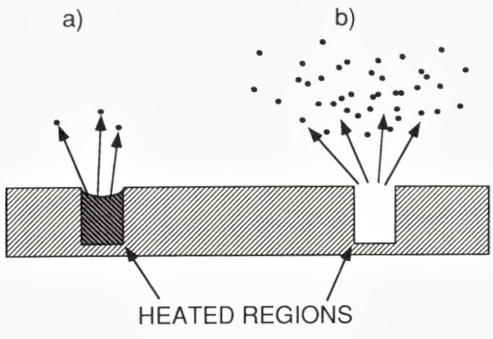

Figure 4. Schematic diagrams of thermal desorption mechanisms. a) Activated desorption (i.e. evaporation); b) Bulk desorption after an irreversible transition to the gas phase.

equal to the radius of the target molecule. The integral diverges for $i_{\min} = 1$, but in practice, fits to data have yielded $i_{\min} > 1$. For large $(dE/dx)_e$, the predicted stopping power scaling is $Y \propto (dE/dx)_e$. This scaling stems from the dependence of $\varepsilon(r)$ on r and $(dE/dx)_e$, as shown in eq. 2 above. For smaller $(dE/dx)_e$, a steeper scaling is predicted, $Y \propto (dE/dx)_e^n$, with $n > 1$.

Hedin et al. (1985) successfully employed hit theory and the ion track model to account for the $(dE/dx)_e$ dependencies of ion yields for a number of organic substances. Shown in fig. 3 is a plot of the $(dE/dx)_e$ dependence of the desorption of ions of valine monomers (117 u) and clusters (up to the tetramer). The ion yield is divided by $(dE/dx)_e$ and plotted against $(dE/dx)_e$. The rising and saturating behavior with respect to $(dE/dx)_e$ occurs just as predicted by the ion track model. If the minimum number of hits causing desorption, $i_{\min}$, is employed as a fitting parameter, then it turns out that the larger the cluster, the larger $i_{\min}$. The conclusion is that more massive target molecules require a greater number of hits in order to be desorbed.

Despite the success of the ion track model in describing ion yield scaling with $(dE/dx)_e$, the general usefulness of the model seems limited. It does not account for the asymmetric ion emission patterns observed by Ens et al. (1989) in off-normal MeV ion incidence experiments. The model makes reference to ionization only through a proportionality constant, so it cannot account for the observation by Hedin et al. (1987) that the yield of small neutral biomolecules obeys a cubic scaling law, $Y \propto (dE/dx)_e^3$ (for bulk desorption, a possible dependence of Z_{avg} on $(dE/dx)_e$ could be considered, however). The similarity noted by Ens et al. (1989a) and others between secondary ion mass spectra from keV and MeV atomic-ion-bombarded organic samples must be regarded as a mystery from the standpoint

of the ion track model, considering that very few secondary electrons are emitted in keV atomic ion impacts. Finally, the most useful aspect of the ion track model is that it may be regarded as a description of the small amount of ionization which occurs along with the dominant desorption of neutrals. However, it may be anticipated that the neutral desorption process will modulate the ionization and neutralization processes, and the ion track model fails to address this issue.

4 Thermal Models of Desorption

Thermal models of desorption, which may be important in a variety of types of particle-surface interactions, are easily described qualitatively. After an ion impact, energy is deposited locally within a small volume. As a result of either collisions or coupling of electronic energy into the nuclear coordinates, target particles receive a certain amount of kinetic energy. If nearly every particle in the energized region acquires significant kinetic energy, then the energized region is referred to as a 'thermal spike' or 'elastic spike' and may be characterized by a temperature T. Once created, a thermal spike evolves spatially over time due to heat conduction: $T = T(\mathbf{r}, t)$. The energized region becomes wider but also cools, finally diluting completely.

Two mechanisms by which desorption occurs in response to a thermal spike are shown schematically in fig. 4. The first mechanism is activated desorption, or evaporation from the heated region on a molecule-by-molecule basis. The second mechanism is bulk desorption, in which the energized region of the target spontaneously vaporizes and is emitted all at once. Below, these two desorption mechanisms are described along with their possible areas of applicability.

4.1 Thermally Activated Desorption

The evaporative approach to desorption begins with the heat conduction equation:

$$\boldsymbol{\nabla} \cdot \{\kappa(T) \boldsymbol{\nabla} T\} = C(T) \frac{\partial T}{\partial t}. \tag{5}$$

Here, $\kappa(T)$ is the thermal conductivity and $C(T)$ is the specific heat of the target material. In principle, both quantities may be a function of temperature, and in turn the temperature will be a function of space and time: $T = T(\mathbf{r}, t)$. For a cylindrical track geometry, appropriate to the case of an MeV atomic ion impacting on an organic target and depositing energy electronically, Mozumder (1969) has given an often utilized solution to the heat conduction equation:

$$T(r, t) = \frac{T_0}{1 + 4\delta t / r_0^2} \exp\left\{ \frac{-r^2}{r_0^2 + 4\delta t} \right\}. \tag{6}$$

In this solution, r is the perpendicular distance from the axis of the track, t is the elapsed time after incidence of an ion, $\delta = \kappa/C$ is the thermal diffusivity, and both κ and C are assumed to be independent of temperature. A spatially narrow Gaussian distribution in initial temperature is assumed with initial temperature at the center of the ion track T_0 and initial width r_0. T_0 and r_0 are related as follows:

$$T_0 = \frac{1}{\pi \rho C_v r_0^2} \left(\frac{dE}{dx} \right)_e . \tag{7}$$

In this formula, ρ is the mass density of the target, C_v is the unit mass heat capacity, and $(dE/dx)_e$ is the electronic stopping power. The general nature of the solution shown in eq. 6 is that, away from the region of initial excitation, there is a temperature 'pulse' which then decays as the heat energy flows to infinity.

A general expression for the evaporative desorption yield due to a thermal spike is written as a surface integral:

$$Y = \int_0^\infty dt \int_0^\infty 2\pi r dr \Phi[T(r,t)]. \tag{8}$$

Here, Φ is the thermally activated flux of particles evaporating from the surface, which depends on the local temperature. A typical choice for Φ is the expression for the flux of an ideal gas evaporating at constant density across a planar surface barrier, calculated from the Maxwell-Boltzmann law:

$$\Phi = \frac{n_M kT}{\sqrt{2\pi MkT}} \exp\left(-\frac{U}{kT} \right) . \tag{9}$$

But sometimes the simpler Arrhenius form is employed: $\Phi \propto \exp(U/kT)$. U is the surface binding energy, n_M is the number density of molecules, M is the molecular mass, and k is the Boltzmann constant. The scaling of Y with $(dE/dx)_e$ is discussed generally by Johnson & Evatt (1980) and Johnson (1987). When a 'delta function' or narrow initially energized region is assumed (r_0 and U/kT_0 small), then the central result of the cylindrical thermal evaporation model is $Y \propto (dE/dx)_e^2$. On the other hand, if the track has a larger initial width, then $Y \propto (dE/dx)_e^2$ only at high values of $(dE/dx)_e$; at lower values, Y is a more rapidly varying function of $(dE/dx)_e$.

The above solutions pertain to the special case of cylindrical tracks (usually associated with energy deposition by MeV atomic ions) and temperature-independent κ and C. However, solutions assuming spherical geometry and/or temperature-dependent κ and C have also been presented by Vineyard (1976), Johnson & Evatt (1980), Sigmund & Claussen (1981), Urbassek & Sigmund (1984), and many others. As noted for example by Sigmund (1974), the gradients in the energy density

deposited by an incident ion can be so large that the concept of local thermodynamical equilibrium is not valid. In response to this objection, Johnson et al. (1991) have given an elastic spike formalism which does not assume local thermodynamical equilibrium. In this case, instead of a local temperature $T(\mathbf{r}, t)$, a local energy density $\varepsilon(\mathbf{r}, t)$ is employed in the diffusive description. A modified expression for the evaporative flux must be employed, but $Y \propto (dE/dx)_e^2$ scaling still results.

Lucchese (1987) has presented an alternative thermal desorption model, based on a cylindrical initial excitation, which gives a different high $(dE/dx)_e$ scaling law: $Y \propto (dE/dx)_e^1$. The main modifications to the above theory are that a rate equation approach is employed, and that only molecules from the first monolayer are assumed to be capable of being thermally desorbed. If $F(\mathbf{r}, t)$ is the fraction of first monolayer molecules remaining at distance r and time t, then one may write the following activated rate equation which comes from transition state theory:

$$\frac{dF(r,t)}{dt} = -\frac{\Omega_0}{2\pi} \exp\left\{-\frac{U}{kT(r,t)}\right\} F(r,t). \tag{10}$$

Ω_0 is the frequency characterizing the molecule-surface bonding. Employing one of the standard expressions for $T(\mathbf{r}, t)$, eq. 10 can be integrated in order to find the values of F after the thermal spike has dissipated. The predicted desorption yield is given by the following surface integral:

$$Y = \sigma \int_0^\infty 2\pi r dr \{1 - F(r, t{=}\infty)\} \tag{11}$$

where σ is the surface number density of molecules. The ion yield is modelled by an additional multiplicative factor which is the fraction of desorbed molecules leaving in the ionized state. Lucchese (1987) has extended this model in several respects, but the key point is as follows. The combination of an assumption of only surface monolayer molecules being desorbed and the exponentially activated nature of the desorption together mean that: for each ion impact, there will be a relatively abrupt boundary between the region in which nearly all surface molecules have been desorbed and the region in which almost no surface molecules have been desorbed. Thus, a 'platter' or 'raft' of molecules is desorbed. If one performs a dimensional analysis of the heat diffusion equation, eq. 5, and takes cognizance of eq. 7, one may see that the platter area turns out to be roughly proportional to $(dE/dx)_e$ (for large enough $(dE/dx)_e$), and therefore so does the desorption yield: $Y \propto (dE/dx)_e^1$. Unfortunately, no reason is given why it should be anticipated that thermal desorption of ions and/or neutrals would take place only from the surface monolayer.

One key objection to the thermal spike model with evaporative desorption is this: If the excited region is in local thermal equilibrium, then by the time a

molecule acquires enough translational thermal energy in order to evaporate, it has also acquired more than enough internal energy to dissociate. This problem has been discussed by Williams & Sundqvist (1987) and others. Although it is not clear if this objection can be successfully overcome, Lee & Lucchese (1989) have attempted to show that thermal desorption with 'cool' internal modes can occur. They have calculated stochastic classical trajectories of a model system in response to a temperature pulse such as that described by eq. 6. The model system consisted of a linear molecule bound perpendicularly to a surface. The molecule consisted of 40 'units' arranged in a linear chain, each unit with mass 15 u, and with the bottom unit representing the surface. Binding among the top 39 units was strong compared with the binding between the surface (first unit) and the adsorbed molecule (via the second unit); the surface bond was also characterized by a low vibrational frequency. The surface unit was subjected to a stochastic force of magnitude and duration in accordance with the thermal spike model, and the internal energy of the top 39 units was monitored as a function of time. The internal energy of the adsorbed molecule remained low and was seen to increase only slowly on the time scale of complete dissipation of the thermal spike.

Lee & Lucchese (1989) employed a very similar model setup in order to monitor the center-of-mass motion of the adsorbed molecule with respect to several atoms representing the substrate. During thermal excitation, the substrate was evidently perturbed by large fluctuations which succeeded in 'pushing away' and eventually desorbing the molecule. The authors conclude that if molecules are bound to a substrate by relatively weak, low frequency bonds, coupling to the translational desorption mode takes place efficiently while coupling to the internal modes takes place only inefficiently. They argue that desorption of a molecule by thermal means is possible without significant fragmentation, as long as equilibrium between translational and internal modes is never achieved on the timescale of desorption.

Applications of activated desorption thermal spike models are many and varied, and it is difficult to give a comprehensive list of appropriate references. However, a few highlights can be mentioned. For example, Ollerhead et al. (1980) proposed a simple thermal spike model to account for MeV ion-induced desorption from solid Xe, and Seiberling et al. (1980) employed the thermal spike model to account for MeV-ion-induced desorption of UF_4. The latter authors suggested a specific mechanism for the initial production of localized heating: a Coulomb explosion, occurring over some time during which ions are left mutually exposed in the infratrack. The thermal spike model can explain much of the data on sputtering of frozen small-molecule gases, as summarized by Johnson (1987, 1990) and Johnson & Sundqvist (1992).

Considering MeV atomic ion bombardment of organic insulators, Macfarlane (1982, 1982a) and Macfarlane & Torgerson (1976, 1976a) were among the first to

suggest that a thermal spike mechanism might be involved in the observed desorption phenomena. These authors also correctly pointed out that the applicability of the thermal spike mechanism depended strongly on the prospect that the internal modes of the desorbed molecules would fail to be in thermal equilibrium with the translational modes, so that fragmentation would not be overwhelming.

The observed stopping power dependencies for both ion and neutral small molecule desorption yields, as far as these are known, can be compared favourably to the predictions of evaporative thermal spike models. Lucchese managed to generate a thermal model which accounted for the $(dE/dx)_e$ dependence of positive ion yields (and in one case negative ion yields too). The model, discussed above, gave a stopping power dependence $Y \propto (dE/dx)_e^1$ for high $(dE/dx)_e$, and the excellent fits which were achieved are shown in fig. 3 for monomers and clusters of the amino acid valine. For lower $(dE/dx)_e$, both data and model show a steeper than linear stopping power scaling. For the amino acid leucine, Hedin et al. (1987) have reported a neutral sputtering yield stopping power scaling $Y \propto (dE/dx)_e^3$. Since the generality of this result is not known, it may turn out that the leucine neutral yield data are also described by the evaporative thermal spike model. If this is true, however, one would predict that for higher but so far untested values of $(dE/dx)_e$, $Y \propto (dE/dx)_e^1$ for neutral leucine desorption. Of course, the general applicability of the evaporative thermal spike model in explaining MeV atomic ion induced desorption of small organic molecules requires that the different measured stopping power scaling of ionic and neutral yields over the same $(dE/dx)_e$ range be convincingly explained. This seems difficult, unfortunately, since these models do not specifically address the ionization mechanism except through an overall proportionality factor.

MeV atomic-ion impact-induced ejection of larger organic molecules, such as proteins, is not well described by the evaporative thermal spike model. This follows mainly from measurements of radial velocity and ejection angle distributions for ions. Evaporative thermal spike models predict an approximate $\cos\theta$ polar angular distribution, whereas Ens et al. (1989), Moshammer et al. (1990) and Moshammer (1991) have found many instances in which both positive and negative large desorbed molecular ions are ejected strongly in off-normal directions. Off-normal ejection is more easily explained employing a pressure-pulse model, discussed below. Unfortunately, it is not known experimentally whether the neutral molecular sputtering yields display similar angular ejection patterns to those of the ion sputtering yields, though the molecular dynamics simulations of Fenyö et al. (1990) based on the pressure-pulse idea seem to suggest that this would be so.

Evaporative thermal spike ideas have been successfully employed to rationalize features of keV to MeV heavy cluster ion bombardment of carbon and organic insulators. Matthew et al. (1986) have employed a thermal spike model in an attempt

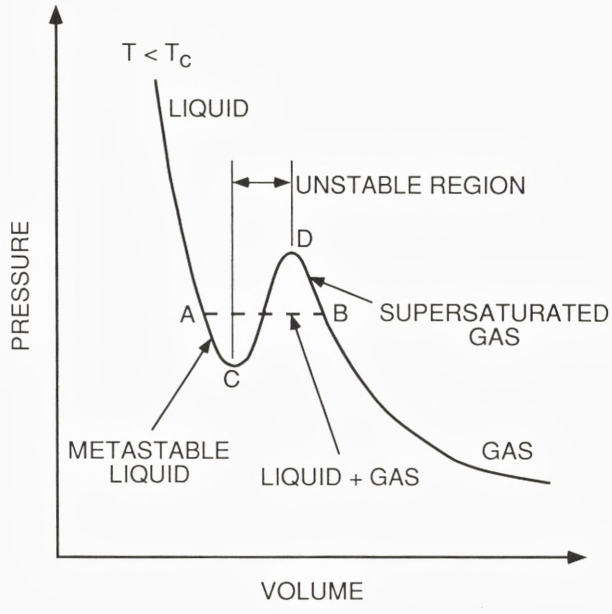

Figure 5. Pressure-volume curve for a material exhibiting a liquid-to-gas phase transition. Segment A-C represents a metastable liquid; segment D-B represents a supersaturated gas; and segment C-D represents an absolutely unstable state of the liquid, characterized by an irreversible transition to the vapor phase.

to understand the formation of craters in thin carbon films under impact of cluster ions of the form $(H_2O)_nH^+$, where n ranges from 25 to 150. Typical impact kinetic energies were 100 to 300 keV. Briefly, an impacting cluster was assumed to deform into a flat 'disc' upon impact, and, assuming a constant cluster stopping power $(dE/dx)_c$, the initial temperature profile of an approximately cylindrical thermal spike was calculated. The heat diffusion equation was employed to calculate the spatial and temporal dilution of heat energy, and the evaporative model described above was used to calculate the number of evaporated carbon atoms. The volume of excavated material was compared to the observed crater volume. One important uncertainty in this model is the value of the stopping power suitable for describing the interaction of an impacting cluster with the target. However, the values of $(dE/dx)_c$ required to explain the observed crater size were within a factor of two of a simple estimate of cluster stopping power based on a simple atomic picture. Some subtleties that enter into the determination of the stopping power of a cluster are discussed by Sigmund (1989).

Ledbetter et al. (1987) bombarded a sample composed of tobacco mosaic virus

(TMV) with cluster ions of the form $(H_2O)_nH^+$. Typical impact kinetic energies were 100 to 300 keV. By employing transmission electron microscopy, the orderly excision and complete disappearance of 'slices' of TMV with no accompanying left-over debris whatsoever was observed. The edges of the excised slices appeared to be flat and were perpendicular to the axis of the cylindrical TMV. The authors pointed out that the structure of TMV consists of a number of slice-like 'gyres' which are relatively more weakly bound to each other than they are internally bonded. The material that had taken up the volume of a typical crater had been composed of up to six gyres, whereas the size of the impacting cluster is only a fraction of the size of one gyre. The central idea that emerges is as follows: Cluster impact produces a local high temperature thermal spike of restricted spatial extent; the thermal energy diffuses much more efficiently within a gyre than across the boundary between gyres. Consequently, evaporation proceeds efficiently, even across several gyres, until the thermal energy diffusing up to one gyre-gyre boundary is suddenly reduced below a certain threshold. Thereafter, very little energy is transmitted, and the evaporation abruptly ceases with the result that the final crater shape is determined by the shape of the gyre-gyre boundary. The evaporative thermal spike model may thus serve as an effective rationalization for the formation of craters in cluster-ion bombarded TMV.

4.2 Thermally Induced Bulk Desorption

The term 'bulk desorption' refers generally to events in which locally deposited energy causes an abrupt transition of a volume of solid or liquid to the gas phase, after which the gassified material escapes from the surface. This desorption mechanism is sometimes referred to as 'gas-flow' or 'phase-explosion' desorption. A number of approaches have been taken to modelling bulk desorption processes. Sunner et al. (1988) have employed a simple thermodynamic picture; Urbassek & Waldeer (1991) and Shiea & Sunner (1991) have employed molecular dynamics simulations; and several authors have performed analytical treatments of adiabatic expansion, for example: David et al. (1986), Urbassek & Michl (1987), and Kelly (1990). These treatments are reviewed here, although applications of these theories to desorption from organic targets are sparse.

The simple thermodynamical picture of bulk desorption begins with a pressure-volume (PV) diagram for a material which exhibits a liquid-gas phase transition. A schematic PV diagram is shown in fig. 5. For temperatures below the critical temperature, T_c, as the pressure is decreased by increasing the volume, there is a range of volumes for which the pressure remains constant (denoted by the dashed line in fig. 5). At this stage, due to heterogeneous nucleation (i.e. the presence of some dust or other impurities in the liquid), the liquid evaporates (boils) as the

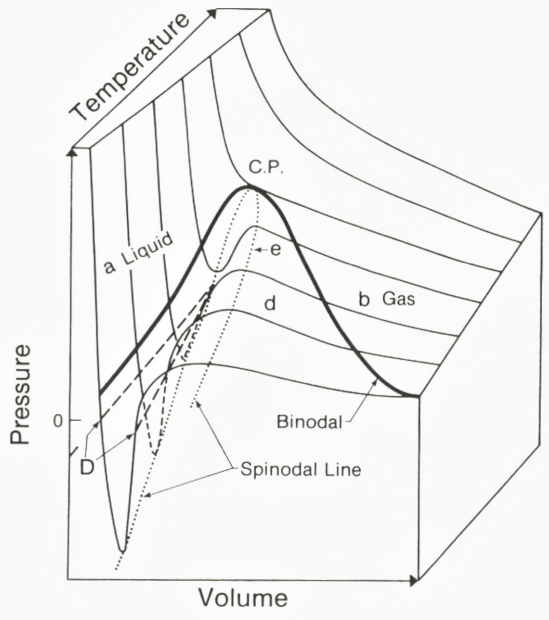

Figure 6. Pressure-volume-temperature surface showing all thermodynamic states available to a simple one-component system. The surface includes the metastable thermodynamic states. The spinodal line encloses the states which are unstable and lead to spontaneous vaporization. The phase explosion model states that an ion impact drives the system from the left-most point of D to the spinodal, leading to vaporization and bulk desorption. Reprinted from Sunner et al. (1988) by permission.

volume increases, keeping the pressure constant. When all the liquid has evaporated, the pressure again decreases as the volume increases. A reverse behavior occurs upon compression of the gas.

In the absence of heterogeneous nucleation, a different behavior occurs. Overexpansion past the volume at which the liquid normally would have begun to evaporate fails to induce evaporation, giving a metastable liquid. Overcompression past the point at which the gas normally would have begun to condense fails to induce condensation, giving a metastable or supersaturated gas. As shown in fig. 5, there is a bit of 'forbidden' PV curve which joins the metastable liquid and supersaturated gas states. This connecting piece, shown in fig. 5 as segment C-D, is characterized by the following relation:

$$\left(\frac{\partial P}{\partial V}\right)_T \geq 0. \tag{12}$$

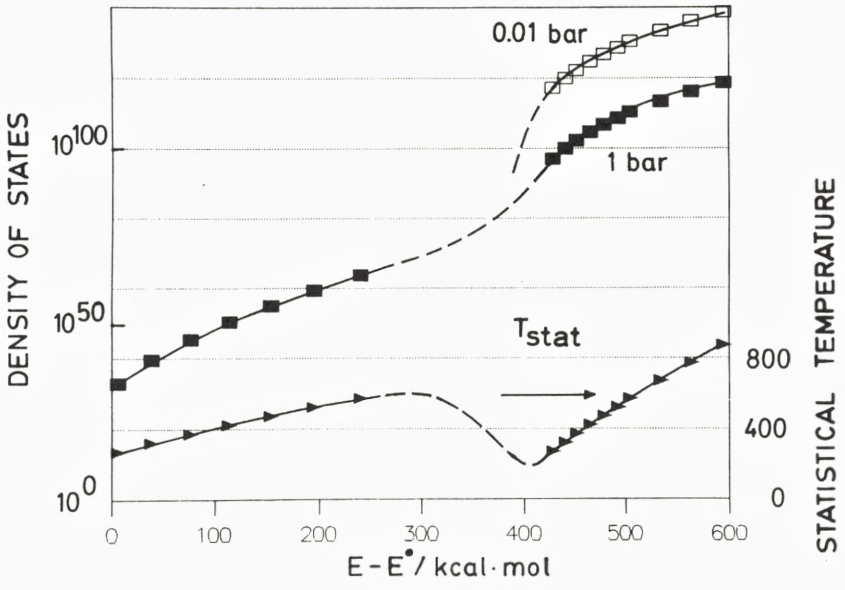

Figure 7. DOS and T_{stat} plotted against internal energy for ten H_2O molecules. A region of log(DOS) characterized by positive curvature is unstable by entropy considerations and undergoes a spinodal transition to vapor and clusters. Reprinted from Sunner (1990) by permission.

According to this relation, the liquid is absolutely mechanically unstable, and a spontaneous phase transition occurs to the 'spinodal' form consisting of a combination of vapor and clusters. This scenario is discussed by Zeldovich & Todes (1940).

Sunner et al. (1988) show a typical pressure-volume-temperature (PVT) surface characterizing a single component system. An example of such a PVT surface is shown schematically in fig. 6. They consider the case of liquid glycerol, a commonly employed matrix for FAB (keV atom impact). Under vacuum conditions, glycerol is a metastable liquid which only very slowly evaporates. It is argued that an incident atomic particle deposits energy, driving up the local temperature. If the heated material reaches the spinodal line at which the liquid becomes unstable against vaporization, the resulting gas is ejected into vacuum, entraining any analyte molecules that have been dissolved in the glycerol and delivering these to the gas phase as well. Pre-formed ions in the solution, ions charged statistically during desorption, and neutral analyte molecules charged during gas phase interactions with matrix ions in the selvedge, are all available for detection in FAB secondary ion mass spectroscopy. The sudden decompression of the gas during ejection gives

rise to a strong cooling effect, and a low degree of internal energy and low fragmentation are expected in the desorbed molecules. Sunner et al. (1988) suggest that the duration of high temperature conditions is at most of the order of 10^{-9} sec. The overall scenario thus parallels that which is thought to occur during matrix-assisted laser desorption.

Two criticisms may be levelled at the above treatment. First, the use of PVT diagrams is only valid for systems in thermal equilibrium, whereas the desorption system may be far from equilibrium. Second, the desorption system may be too small for the principles of bulk thermodynamics to be valid. In response to these criticisms, Sunner (1990) has provided an alternative treatment based on statistical thermodynamics. In this case, the density of states (DOS) for a microscopic ensemble of ten water molecules is back-calculated from entropy and enthalpy values for bulk water. The curve DOS vs. E (total energy) is plotted semi-logarithmically in fig. 7. At the left and right of the plot are the water liquid and gas phases respectively, and for each phase, the statistical temperature (inverse slope of a log(DOS) vs. E plot) increases with increasing total energy. However, there is a range of energies for which the log(DOS) vs. E curve would clearly have a positive curvature, displaying a decreasing temperature as the total energy increases. This is the mechanically unstable region discussed above in connection with a PVT diagram, but now the instability can be understood through an entropy argument. Since log(DOS) is the entropy, then at a point at which the log(DOS) vs. E curve has a positive curvature, the entropy always increases if the system breaks up into part gas phase and part liquid phase. Therefore, the break-up is spontaneous, and for a certain total energy density, liquid water vaporizes and ejects clusters in a spinodal transition. Sunner (1990) also points out that, during the phase explosion, energy may flow from internal vibrational states of water (which molecules are individually stable independently of the stability of the phase in which the molecules reside) to the translational modes, resulting in 'cooler' molecules and clusters, and faster (but more directed) ejection.

Molecular dynamics simulations have also been employed to gain insight into bulk desorption processes. Such methods have the advantage that, in principle, only microscopic interaction details need be specified, and the conditions of equilibrium or lack thereof can be demonstrated by sampling the internal kinetic energy distribution as a function of time. Unfortunately, classical dynamics simulations tend to be limited to the cases of solids composed of atoms and small molecules.

Urbassek & Waldeer (1991) and Waldeer & Urbassek (1993) have performed classical dynamics simulations on a condensed argon solid collisionally energized by a 1 keV argon atom. Results of their study are shown in figs. 8 and 9. The state of the system is monitored by noting in what form material escapes, and by sampling the kinetic energy spectra of atoms in the solid as a function of time.

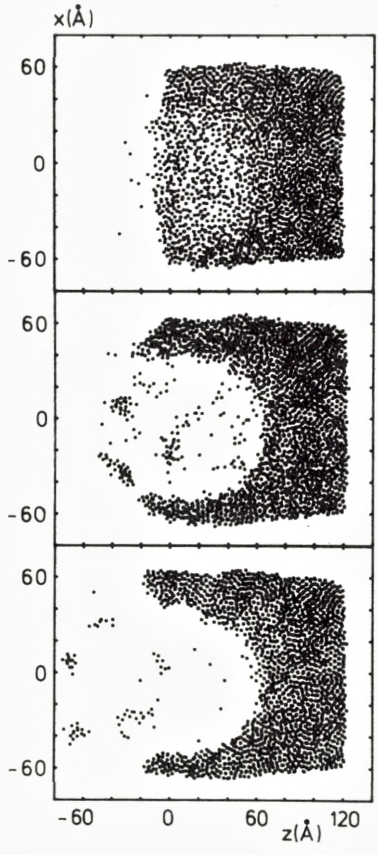

Figure 8. Crater formation in an argon solid after incidence of a 1 keV argon ion. Top frame: 3.2 psec after impact. Middle frame: 13.8 psec. Bottom frame: 24.7 psec. Extensive clustering is apparent. Reprinted from Urbassek & Waldeer (1991) by permission.

At very early times after the ion impact, the internal kinetic energy distribution is mainly the same low temperature Maxwell-Boltzmann distribution which characterized the solid just before the ion impact, but with an added collision cascade 'tail' at high energies displaying the usual E^{-2} scaling. For slightly later times, but still before many atoms have left the target, the kinetic energy spectrum indicates that the system is far from equilibrium. This spectrum cannot be fit even by a summation of two Maxwell-Boltzmann models. At comparatively late times, after hundreds of atoms have been sputtered, the internal kinetic energy distribution is again a relatively low temperature Maxwell-Boltzmann distribution. The max-

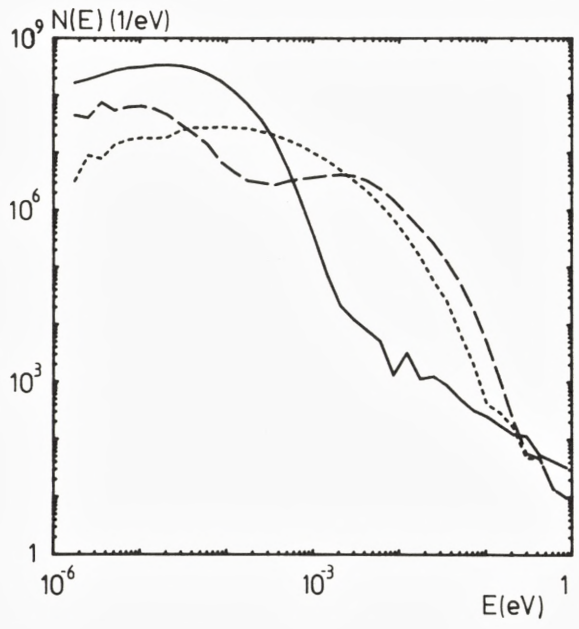

Figure 9. Kinetic energy spectrum of argon atoms in the solid shown in fig. 8. Solid line: 0.14 psec after impact. Dashed line: 3.2 psec. Dotted line: 24.7 psec. Note marked lack of equilibrium at 3.2 psec. Reprinted from Urbassek and Waldeer (1991) by permission.

imum temperature during the whole desorption process is never even as high as the critical temperature of liquid argon, and the condition of high kinetic energy density lasts only about 10 psec. The extensive clustering observed in the sputtered plume is indicative of rather low internal energies of sputtered particles. Although a thermodynamical picture does not hold in detail throughout the desorption event, the classical dynamics and thermodynamics pictures yield the same conclusions: a large portion of the target is vaporized and ejected as a gas, with marked clustering accompanying the gas expansion. Although the simulation is aimed at assessing the role of bulk desorption in the case of particle-excited rare gas solids, there is no reason in principle why the same concepts should not be applicable to a variety of organic targets as well.

Shiea & Sunner (1991) have also performed classical dynamics simulations of bulk desorption. They considered a very low energy projectile incident on an two-dimensional atomic lattice and made plots of kinetic energy density as a function of time and space. They plotted an internal energy ('temperature') history for a region of the solid near the incident ion impact point. Just after projectile impact,

there is a temperature pulse lasting less than 1 psec, and this is attributed to the passage of a shock wave through the lattice. Next a slower temperature pulse lasting 2 or 3 psec is observed and this evidently causes a weak spinodal transition of the sort which was predicted by thermodynamic theory and discussed above: a transformation of the lattice to an assortment of isolated atoms and 'filaments' of atoms, or clusters. If molecules are included in the lattice, some of these are ejected intact.

A number of authors have attempted analytical descriptions of the dynamics of bulk desorption, although again these treatments are aimed at clarifying sputtering mainly of atomic solids. Urbassek & Michl (1987) have modelled the bulk desorption process in terms of collision-free molecular flow in three dimensions, a procedure they claim is a good approximation to the correct description in terms of unsteady adiabatic expansion. Noting that the collision-free molecular flow formalism cannot possibly model the dissipation of energy by thermal conduction, they add a nonconservative force field to simulate this heat dissipation. Finally, the possibility of recondensation is included by halting the gas flow out of the crater when the temperature falls below a certain critical value, taken arbitrarily to be the sample boiling point. The derivations of and resulting expressions for the sputtering yield and the axial kinetic energy spectrum are given but they are detailed and are not repeated here. The model axial kinetic energy spectra, when fitted with parameters suitable for describing the spatial extent of collisional excitation by a keV atomic ion incident on a solid rare gas target, were able to account for the low kinetic energy sputtered atom yield, which is typically much higher than can be accounted for by the simple collision cascade model. As noted above, these same concepts may well also be applicable to organic targets.

Balaji et al. (1990) have given a simplified derivation of the total desorption yield calculated by Urbassek & Michl (1987). They employ the evaporative thermal spike yield equation, eq. 8, with an expression for the flux appropriate to the situation of an ideal gas passing across a plane with no binding potential: $\Phi(T) \propto T^{1/2}$. They then assume that the temperature drops in time according to eq. 6 but with the exponential part held at exactly one, i.e. they consider only regions of the sample very close to the ion impact track and assume a constant initial track radius as did Sigmund & Claussen (1981). The time integral in eq. 8 is then effectively simplified and parametrized in terms of temperature, and upon including a critical condensation temperature, an expression for the sputtering yield is obtained which is the same as that obtained by Urbassek & Michl (1987).

Kelly (1990) has adapted the analytical solution for one-dimensional unsteady adiabatic expansion to the case of keV atomic ions incident on various frozen gases. The modelled situation is that of a 'plug' of hot material. The size and temperature of the plug are determined by the parameters of the material and the impacting

ion. If the temperature of the plug exceeds the critical temperature, the material turns into a hot dense gas which escapes. The situation in which a gas is suddenly released from a hole or cavity is described by equations governing adiabatic expansion in the continuum limit, which have been specified and solved. The essence of the solution is that, at some point in time, the density of the escaping gas has decreased to the point at which collision-free molecular flow occurs. At this point, the dominant fraction of the gas has a number of well-defined properties. In particular, the temperature of the gas is uniform, and its flow speed is linear in distance from the bottom of the evacuated plug but achieves a well-defined maximum value. The axial kinetic energy spectrum consists of the Maxwellian form, superimposed on a flow, and integrated over the entire range of flow velocities in the plume. The analytic result for the energy spectrum is complex but is similar in form to a single Maxwellian velocity distribution superimposed on a single flow velocity. Sputtering yields predicted in this gas flow model greatly exceed the yields predicted from collisional sputtering. It is suggested that, though the present model is one-dimensional in nature, in a three-dimensional measurement additional information is available from measurements of the angular distributions of sputtered particles, and the higher the gas flow velocity, the narrower the angular distributions are likely to be. Although these ideas have been applied mainly to the case of ion-bombarded frozen gases, it is likely that application to certain organic targets could also be fruitful and should be considered.

For applications, the case of keV atomic particles incident on glycerol is first considered. Glycerol is a commonly employed matrix material for FAB secondary ion mass spectroscopy measurements. The sputtering yield of glycerol under keV atomic ion bombardment is thought to be high, although admittedly the technical problem of accounting for evaporation during the measurement is a taxing one. Barofsky & Barofsky (1986) and Barofsky et al. (1991) have measured sputtering yields in the range 1000 to 4000 for a variety of ions incident on liquid glycerol, for example 10 to 30 keV Bi^+, In^+, and Ga^+. Wong et al. (1985) have measured comparable sputtering yields for 6 to 10 keV Xe atoms incident on glycerol. A bulk-desorption or gas-flow model provides an attractive rationalization for such high sputtering yields.

Just as the use of a matrix material revolutionized the technique of laser desorption for biomolecular mass analysis (Karas & Hillenkamp, 1988), so did the use of matrix materials like liquid glycerol revolutionize the technique of FAB mass analysis (Barber et al. 1981, de Pauw, 1986). Compared to solid matrices, the use of liquid matrices can yield mass spectra characterized by greater intensity and a lower degree of fragmentation. Part of this improvement is due to renewal effects absent for solid targets: in the liquid, ion-induced damage at the surface is in effect 'rinsed away' into the bulk of the liquid. However, another part of the

improvement may be caused by the gentle ejection of analyte molecules entrained in a plume of desorbing matrix molecules. Significant cooling occurs, as discussed above, and this results in lower fragmentation rates. This cooling has been observed by Hoogerbrugge et al. (1988), who performed photo-ionization measurements on sputtered glycerol molecules. By monitoring fragmentation patterns and comparing to similar patterns measured for heated glycerol gas, they concluded that the desorbed glycerol molecules have considerably lower internal energy then they had in the liquid phase prior to sputtering. Such cooling effects are consistent with the operation of a bulk desorption mechanism in the case of liquid matrices excited by incident ions.

Sunner et al. (1988, 1988a) and Shiea & Sunner (1990) have also employed bulk desorption ideas to explain a number of observations that they have made in connection with FAB. For example, Sunner et al. (1988a) acquired FAB spectra of a variety of matrix substances, listed in order of mass: water, methanol, ethanol, 2-propanol, n-butanol, n-octanol, and glycerol. While extensive clustering is observed in the case of water (and also nitrogen) matrices, the clustering propensity sharply decreases in the order listed. The authors explain this trend in terms of an enthalpy argument. In the case of water, the enthalpy content at the spinodal state is less than what is required to guarantee the creation of an homogeneous vapor phase. Consequently, extensive clustering is observed in the FAB spectra. For 2-proponal, by contrast, it turns out that the enthalpy content of the spinodal state is sufficient to guarantee complete vaporization. In this case, a smaller degree of clustering was observed in the FAB spectra. The applicability of thermodynamic concepts to the FAB desorption process is taken to be in favor of the validity of phase-explosion and bulk desorption ideas.

Shiea & Sunner (1990) monitored FAB spectra as they varied the viscosity of the matrix material by means of changes in temperature and modifications to the matrix solution. They noted that, for a sufficiently great increase in the viscosity, the FAB spectra deteriorated, displaying a large degree of fragmentation and chemical noise. The authors offered the following rationalization for this effect. They assumed that the material in the core region of the collision-cascade induced spike is gassified and is characterized by high internal energy and a high degree of fragmentation. In the case that the surrounding material is characterized by a high viscosity, they supposed that the hot gas is promptly ejected, resulting in poor FAB spectra. In the case that the surrounding material is characterized by a low viscosity, however, they supposed that the surrounding material 'yields' to the increased pressure, delaying the ejection of the hot 'spike' material. Consequently, more of the surrounding material is heated up to the spinodal state and participates in the phase explosion. The result is that a large number of intact, low internal energy molecules are ejected. Under these conditions, excellent FAB

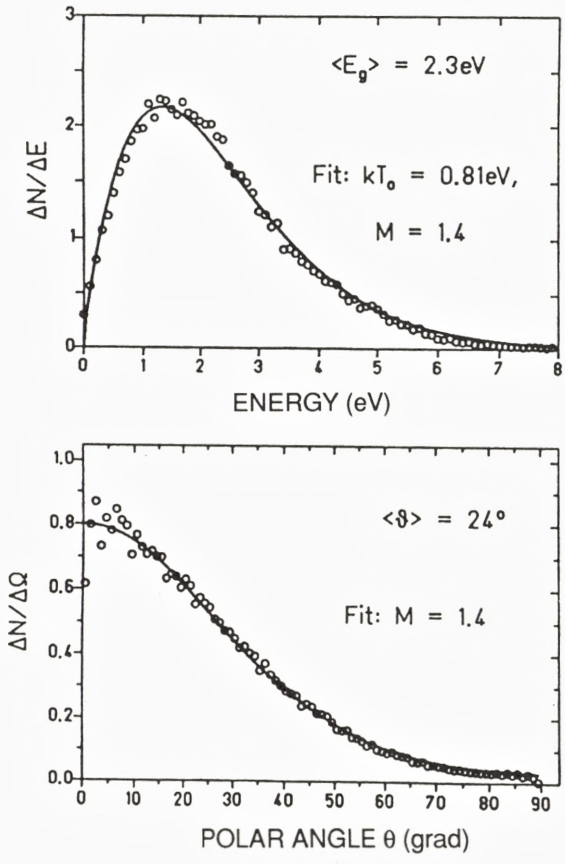

Figure 10. Kinetic energy and ejection polar angle distributions of the $M = 30$ u fragment of valine. Excitation is by ^{252}Cf fission fragments. The solid line is a fit to a Maxwellian velocity distribution with a gas flow velocity superimposed along the surface normal. Reprinted from Moshammer (1991) by permission.

spectra characterized by low noise and strong molecular peaks are obtained.

Much of the discussion of bulk desorption of organic materials revolves around liquid targets. Is a liquid matrix necessary for the occurrence of bulk desorption phenomena for FAB and keV atomic ion irradiation? The answer is not totally clear, but it is possible that bulk desorption could occur in solids. Several items of theory discussed above were based on model solids, after all, and one may suspect that these theories are also applicable at least to solids composed of small organic molecules. Also, there are cases for which SIMS on analytes in the solid phase and

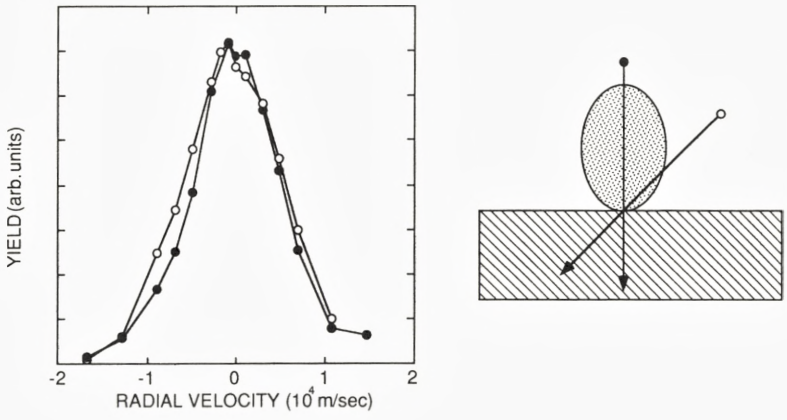

Figure 11. Radial velocity distributions for the $M = 15$ u fragment of insulin, for 0° and 45° angles of incidence. Excitation is by 72.3 MeV ^{127}I ions. The resulting distributions are the same. Adapted from Fenyö et al. (1990a).

in a matrix liquid yielded similar spectra and ion count-rates to within a factor of 10 (see Junack et al., 1986). Finally, solid targets can be a source of rather massive ions, with $M > 10000$ u, suggesting that these ions are ejected gently and with sufficient vibrational cooling to avoid fragmentation.

Although the bulk desorption models provide a qualitative explanation of various features of sputtering by FAB, there is some room for debate whether the model is truly applicable. As discussed in the introduction, it may be suggested that a large fraction of the ejected intact molecules and major fragments are likely to be ejected from outside the region of the target directly excited by the incident ion. An alternative theory of liquid matrix FAB has been offered by Wong & Röllgen (1986), and this theory is discussed below, under the heading 'pressure-pulse sputtering'.

In the area of MeV atomic ion impacts on organic targets, Moshammer (1991) has measured energy- and angle-resolved ejection distributions of fragments of valine ejected by ^{252}Cf fission fragments. The results are displayed in fig. 10. The observed distributions are well accounted for by a Maxwellian superimposed on a supersonic flow characterized by Mach number 1.2, consistent with a simple gas-flow 'ansatz'. The MeV ions, however, create a cylindrical track, and if the gas-flow model is applicable, then there should be evidence of fragments being ejected backwards along the ion track direction in a 'jet-effect'. However, Fenyö et al. (1990a) have noted that this jet effect is conspicuously absent, at least for the CH_3^+ fragment measured, as shown in fig. 11. As the angle of incidence of the impacting ions

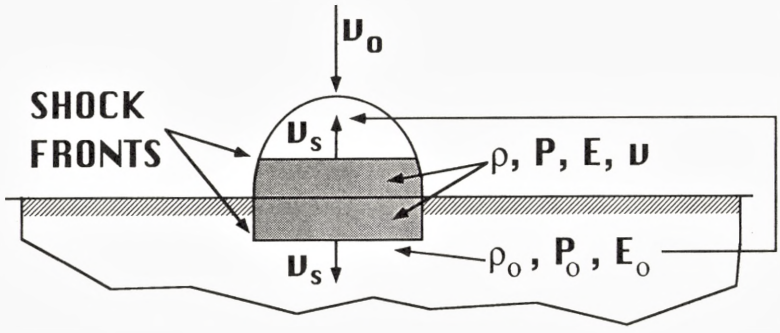

Figure 12. Schematic diagram of shock wave fronts produced as a glycerol cluster impacts a glycerol matrix. For simplicity, a one-dimensional viewpoint is taken. v_0 is the speed of the initial cluster; the other symbols are defined in the text.

was switched between 0° and 45°, no change in the radial velocity distributions was observed. In fact, no jet-effect has ever been observed for pre-existing organic species desorbed from a surface, and consequently it is doubtful that the gas flow model plays a strong role in MeV ion-induced desorption of organic molecules.

5 Shock-Wave Models of Desorption

The incidence of energetic particles onto surfaces can lead to extremely high deposited energy densities. One possible consequence of high energy density and high energy density gradient conditions is that a 'shock wave' may be created which propagates outward from the region of excitation into the surrounding material. Desorption may be caused in several ways. For example, if a shock wave reflects off the surface (vacuum interface) from below, material may be 'mechanically ablated' or 'spallated' by being in effect left behind during the unloading wave. Also, it is possible that shock wave energy may be focused into defects or narrow protrusions sticking off the surface, also leading to direct desorption of a piece of the solid. Finally, after a shock wave passes through a region of a material, this region is left in a heated state, and the excess thermal energy may cause desorption through evaporation or bulk desorption or through response to the energy density gradient (see pressure-pulse discussion below). There is a large body of literature concerning shock wave and hydrodynamic theory (Zel'dovich & Raizer, 1967; Landau & Lifshitz, 1959).

The complex details of the theory are outside the scope of this paper, and thus a qualitative definition of a shock wave is given here. Loosely speaking, a shock

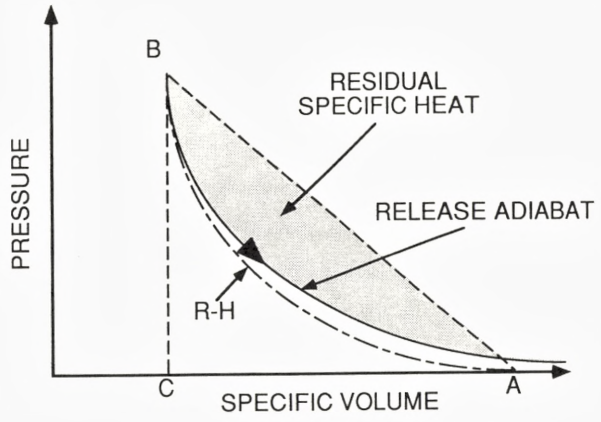

Figure 13. Equation of state for a shocked material. Point A represents the rest or normal state. Points on the Hugoniot, curve R-H, represent final states of the material that can be reached by shock excitation. If the system is excited to point B and subsequently undergoes an adiabatic release or unloading process, then a residual specific heat (heat energy per unit mass) is left whose magnitude is represented by the shaded area shown in the figure. Drawn by Jörgen Ahlbom, Uppsala University.

wave is a relatively narrow propagating mechanical disturbance across which there are distinct changes in thermodynamical parameters like pressure, temperature, and material density. Terms like 'relatively narrow' and 'considerable' are hard to pin down precisely, but narrow means that the width is no more than a few lattice spacings of the material. The shock wave itself propagates with a speed exceeding that of sound in the medium. Supersonic propagation of a mechanical disturbance is a sufficient condition for deducing that the disturbance has a shock-like character.

One shock wave model of desorption is based on the idea that a passing shock wave leaves the material in a heated state. Mahoney et al. (1992) have observed desorption of analyte molecular ions from a glycerol matrix under massive glycerol cluster impacts at three times the speed of sound. The impacting cluster is regarded as a piston which compresses a plug of target material. Shock wave fronts propagate both into the target and back into the incident cluster. These authors have carried out a simple hydrodynamic analysis, utilizing known thermodynamic data on glycerol, to justify that shock wave heating can account for the observed desorption. Their treatment begins with the Rankine-Hugoniot equations applied to the one-dimensional picture of the collision event shown in fig. 12. The Rankine-Hugoniot equations result from applying the principles of conservation of

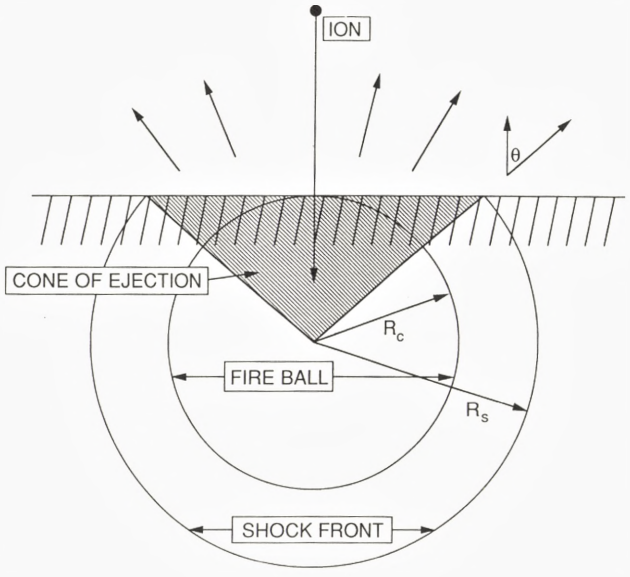

Figure 14. Schematic diagram of a spherical shock wave initiated by a critical energy deposition within a sphere of radius R_c. Based on an ejection criterion discussed in the text, a cone-shaped plug of material, shown in the figure as the shaded volume, is ejected. Adapted from Kitazoe et al. (1981).

momentum, mass, and energy across a shock wave front:

$$\begin{aligned} P - P_0 &= \rho_0 v v_s \\ \frac{V}{V_0} &= \frac{v_s - v}{v_s} \\ E - E_0 &= \frac{1}{2}(P + P_0)(V_0 - V). \end{aligned} \tag{13}$$

In the region behind the shock wave, the pressure is denoted by P, the volume per unit mass is denoted by V, and the energy per unit mass is denoted by E. Corresponding quantities in the unshocked region of the sample are denoted respectively by P_0, V_0, and E_0. The mass density in the unshocked region is $\rho_0 = V_0^{-1}$. v_s is the shock wave speed, and v is the speed of glycerol molecules in the shocked region. (Here and in fig. 12, E and V represent specific energy and specific volume respectively, rather than energy and volume as employed elsewhere in this paper.)

An equation of state for shocked material is shown schematically in fig. 13. In the case of glycerol, the shock wave and molecular speeds are known as a function of

density under shock conditions, and by employing the first two Rankine-Hugoniot equations, an equation of state curve called the Hugoniot may be constructed. Consider initial state A and final state B on the Hugoniot. The area under the straight line segment AB is the shock-induced change in the energy per unit mass. This follows from the form of the third Rankine-Hugoniot equation. The system at state B then undergoes a 'release adiabat' during which compressional potential energy is released. The shaded area shown in fig. 13 represents the leftover specific thermal energy after passage of the shock wave and relaxation of the material. Using the Hugoniot itself as an approximation to the release adiabat, it turns out that for glycerol, the leftover residual specific heat is of the order of magnitude required to vaporize the region of the target excited by cluster impact. Both evaporative thermal spike and bulk desorption mechanisms could be active.

Kitazoe et al. (1981) have performed an analytic hydrodynamical analysis of non-linear sputtering yields for the case of heavy atomic ion bombardment of high-Z materials, again regarding energy dissipated by the shock wave as a cause of sputtering. The geometry treated is shown in fig. 14. The incoming ion is assumed to scatter at some depth R_c, whereupon the scattered atom(s) set up a dense collision cascade or elastic spike. The resulting 'fire ball' has radius R_c. Within this radius, the average energy per volume is approximately

$$\varepsilon \approx \frac{2R_c(dE/dx)}{\frac{4}{3}\pi R_c^3} = \frac{3(dE/dx)}{2\pi R_c^2}. \tag{14}$$

Here, dE/dx is the appropriate stopping power. If $\varepsilon > \varepsilon_c$, a critical value of energy density, then a shock wave is assumed to be created. An expression for the energy per particle, E, behind the shock wave front is given by Landau & Lifshitz (1959) for spherical symmetry. Taking into account energy deposited both as heat and plastic deformation,

$$E(R) \cong \frac{\frac{\varepsilon}{n_A}\left(\frac{R_c}{R}\right)^2}{1 + \frac{3}{2}\sqrt{\frac{2\varepsilon}{Mc^2 n_A}}\log\left(\frac{R}{R_c}\right)}. \tag{15}$$

Here, R is the distance from the center of the fire ball, M is the target particle mass, n_A is the number density of atoms, and c is the speed of sound. Because of the highly compressed nature of the fire ball, $E(R)$ is characterized by a strongly radial macroscopic velocity component, so that the following criterion is employed for ejection:

$$E(R_s)\cos^2\theta = U. \tag{16}$$

R_s is the radial distance from the center of the fire ball to the outermost point on the surface at which ejection can take place, U is the surface binding energy, and

θ is the angle defined in fig. 14. The final ejected volume is assumed to be the conical-shaped volume shown in fig. 14, so that, from geometrical considerations along with eq. 14, the sputtering yield scales as

$$Y \propto R_c^3 \propto \left(\frac{dE}{dx}\right)^{3/2}. \tag{17}$$

The absolute magnitude of the sputtering yield of course depends on θ through eqs. 16 and 15. If the predicted sputtering yield is comparable to or less than the yield predicted by the collision cascade sputtering model, then the shock wave heating model is considered not to be relevant (i.e. the shock is too weak or nonexistent). However, the authors identify a number of cases involving atomic ion bombardment of metal targets for which the model appears to have some validity. Carter (1983) has debated against the relevancy of shock phenomena in describing sputtering from dense elastic collisional spikes, although he admitted the possibility of 'some unspecified collective hydrodynamic motion' occurring early in the spike formation process.

A generally similar viewpoint to the above is taken by Gol'danskii et al. (1975) and Demirev (1988) in describing the interaction of MeV heavy atomic ions with water or organic targets. Solutions are given to equations governing a cylindrically expanding shock wave, appropriate to the geometry of MeV ion interactions with solids. The solutions include expressions for the position of and pressure behind the shock wave front as a function of time. Demirev (1988) noted that for times up to about 50 psec after excitation, and for a radius of 600 Å around the initial track, the resulting pressures correspond to a volume energy density sufficient to desorb typical protein molecules bound by hydrogen or van der Waals bonds.

Bitensky & Parilis (1987) have generated a theory in order to describe desorption of clusters and organic molecules under the influence of spherical and cylindrical shock waves. These authors assume that sputtering occurs by spallation, and they employ a pressure criterion to define the point at which sputtering occurs. Referring again to fig. 14, a conical chunk of material is assumed to be desorbed if

$$P(R_\mathrm{s}) \cos\theta = P_\mathrm{cr} \tag{18}$$

where $\mathrm{P}(R_\mathrm{s})$ is the residual overpressure at radius R_s and P_cr is some critical pressure. If the molecules have radius r_m, then for the molecules to be ejected separately but intact, the following additional conditions must be met:

$$\frac{P_\mathrm{d}}{2r_\mathrm{m}} \geq |\nabla P(r)| \geq \frac{P_\mathrm{cr}}{2r_\mathrm{m}}. \tag{19}$$

In this inequality, the 'pressure' in the molecular volume is related implicitly to the internal energy by hydrodynamical equations, and P_d is related to some internal

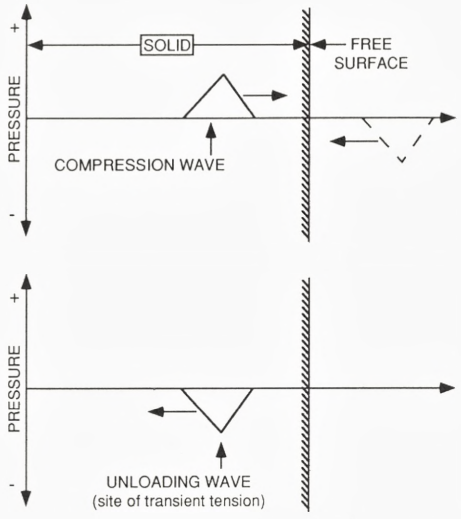

Figure 15. Schematic diagram of an acoustic-like weak shock wave reflecting from the free surface of a solid. A virtual leftward-propagating unloading wave is required in order to preserve the boundary condition that the pressure at the surface be zero at all times. As the compression wave interacts with the free surface, the virtual unloading wave becomes real and causes the solid to experience a transient tensile stress as it propagates into the bulk. The solid may crack or blister and pieces may be ejected. Adapted from Zel'dovich & Raizer (1967).

pressure sufficiently high to cause dissociation of the molecules. As in the treatment of Kitazoe et al. (1981), owing to geometry, the sputtering yield turns out to scale as $Y \propto (dE/dx)^{3/2}$ for sufficiently high (dE/dx).

In the model of Bitensky & Parilis (1987), dissipation is ignored by assuming simple scaling laws for the pressure. (This is analogous to ignoring the logarithmic term in the denominator of eq. 15 so that $E(R)$ obeys a simple geometrical scaling law.) The overpressure then is regarded as causing spallation of a finite-sized chunk of matter from the surface. The concept is illustrated schematically in fig. 15. A weak, acoustic-like shock wave characterized by a pulse-like spatial pressure profile moves towards the free surface. The boundary condition at the surface is that the pressure there is negligible for all time, so the solution to the wave equation involves a counter-propagating negative pressure pulse which is positioned such that this boundary condition is satisfied. Therefore, after the shock wave reaches the surface, an unloading wave characterized by negative pressure propagates down into the solid. Negative pressure is interpreted as a tensile stress, and if this stress is sufficiently large, the material may fracture and the loose pieces of material may

be ejected. These concepts are discussed by Zel'dovich & Raizer (1967).

The detailed scaling law derived by Bitensky and Parilis (1987) was successfully employed to fit the MeV-ion-induced molecular ion desorption results of Hedin et al. (1985), but this scaling law is not consistent with the scaling observed for neutral desorbed molecules by Hedin et al. (1987), $Y \propto (dE/dx)_e^3$. Therefore, ways of improving the performance of the model have been discussed by Bitensky et al. (1989, 1990, 1991) and Parilis et al. (1993). In particular, an alternative assumption about how shock waves arise is considered. If the shock wave is assumed to originate when the energy flux through the boundary defining the originally excited region exceeds a critical value, then $R_S \propto dE/dx$ and the sputtering yield will have a cubic dependence on dE/dx. However, note that an energy flux is directly related to an energy gradient. Thus, the improved version of the shock wave model resembles quite closely the pressure pulse model discussed in the next section. In fact, the Bitensky et al. (1991) expressions for the normal and radial components of 'pressure' and those given by Fenyö & Johnson (1992) for the momentum acquired by a molecule under the action of an energy density gradient are essentially the same. For MeV atomic ions incident on organic targets, calculated spatial distributions of sputtered molecules (Bitensky et al., 1991) are in excellent qualitative agreement with measured spatial distributions of desorbed molecular ions (Moshammer et al., 1990).

Molecular dynamics simulations may profitably be exploited to examine or model shock wave phenomena on a microscopic scale. For example, Holian et al. (1980) have modeled piston-driven shock waves in Lennard-Jones fluids like liquid argon. Robertson et al. (1991) have simulated a steady split shock wave in a solid which undergoes a phase transition. And Wagner et al. (1992) have simulated spallation at high strain rates under shock wave excitation. In all cases tested so far, good agreement is obtained between the simulation results and results from macroscopic continuum mechanics theory. This is remarkable considering that the simulations are based on a microscopic description of the interactions between the particles making up the system.

The use of molecular dynamics simulations for understanding shock effects after excitation of a target by an incident ion does not yet seem to be highly developed. Therefore, only three examples are briefly discussed here. Again the simulation by Shiea and Sunner (1991) is mentioned. They considered an atomic particle incident on a Lennard-Jones matrix. A temperature spike occurring around 0.5 psec after particle excitation was attributed to the passage of a shockwave. It seems that a second temperature spike occurring at 1.5 psec could be attributed to thermal energy remaining after unloading at the surface begins to proceed (in a manner similar to that shown in figs. 13 and 15 but probably differing in some details), but this interpretation is by no means clear. Another example is provided by Fenyö &

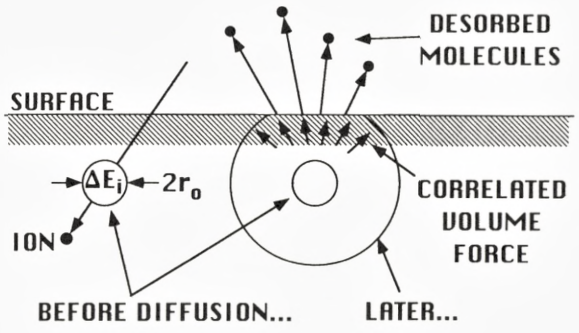

Figure 16. Left: an incident ion creates a localized region of kinetic energy excitation. Right: the motional energy diffuses collisionally. As energy reaches the surface, desorption may occur either by evaporation or in response to the correlated volume force, $\nabla\varepsilon(\mathbf{r}, t)$.

Johnson (1992), who model a Lennard-Jones solid excited by depositing potential energy in a cylindrical core or 'track'. A disturbance propagating to the boundary in less than 2 psec is regarded as being the remnant of a shock wave which was diluted after travelling a distance of only 20 Å. Excess energy is left in the central excited region of the track, and this energy diffuses collisionally, causing pressure pulse desorption after about 5 psec as described below. It is possible that some fraction of the energy initially confined to the track region was due to shock heating. However, in this case it seems hard to rigorously define a shock wave given a space of only 20 Å. Finally, one may refer again to the results of Waldeer & Urbassek (1993), who modeled the sputtering caused by the incidence of an argon ion on an argon lattice. The authors clearly observed shock waves in their simulations but claimed that they did not contribute to the sputtering process.

In the absence of work designed to investigate deliberately and carefully the role played by shock waves in particle desorption, one must regard the concept of shock induced sputtering as being not well developed for geometries in which the shock waves, if they exist, are rapidly degraded to weak acoustic waves. The question of the role of shock waves in particle desorption is still very much open to discussion, and new models are appearing, such as the soliton sound-shock model of Hilf et al. (to be published).

6 Pressure-Pulse Models of Desorption

The highlights of a pressure pulse model of desorption of organic molecules have been presented by Johnson et al. (1989). The essential aspects of the model are

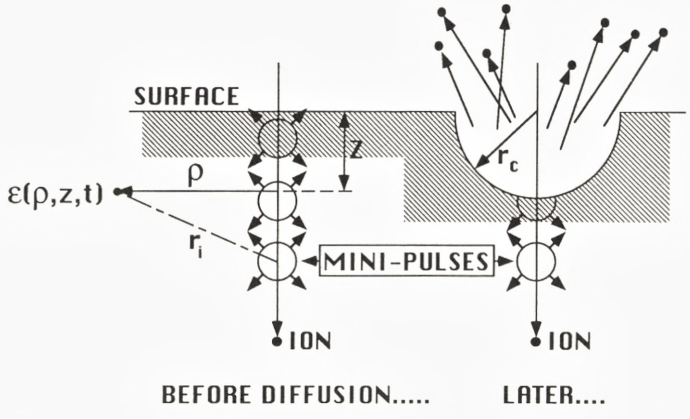

Figure 17. Pressure pulse model applied to a cylindrical ion track. Left: the cylindrical ion track is regarded as being composed of a series of "mini-pulses" spaced by a distance λ. Right: under the action of the correlated volume force, $-\nabla\varepsilon(\mathbf{r},t)$, a half-sphere of the target is ejected. r_c scales linearly with $\Delta E/\lambda \approx dE/dx$.

reviewed here. To start with, an ion traversing a solid is assumed to deposit kinetic energy ΔE_i in a small spherical volume of radius r_0. The kinetic energy could be the result either of a collisional interaction or of an electronic interaction with partial conversion of the electronically deposited energy into kinetic energy. The assumed geometry is shown in fig. 16. The energy is assumed to propagate according to a simple diffusion equation:

$$\nabla \cdot [\kappa \nabla \varepsilon(\mathbf{r},t)] = \frac{\partial \varepsilon(\mathbf{r},t)}{\partial t}. \tag{20}$$

In this equation, κ is the diffusivity, and $\varepsilon(\mathbf{r},t)$ is the volume energy density as a function of spatial coordinates and time. The solution of eq. 20 is:

$$\varepsilon(\mathbf{r},t) = \frac{\Delta E_i}{\pi^{3/2}(r_0^2 + 4\kappa t)^{3/2}} \exp\left(-\frac{r^2}{r_0^2 + 4\kappa t}\right). \tag{21}$$

If $\varepsilon(\mathbf{r},t)/kn_M$ is identified as a local temperature $T(\mathbf{r},t)$, then the result is the thermal spike formalism discussed above but for a spherical geometry. An evaporative desorption yield could be calculated using eqs. 8 and 9.

The existence of a gradient in $\varepsilon(\mathbf{r},t)$ gives rise to a 'volume force': $-\nabla\varepsilon(\mathbf{r},t)$ is the net force per unit volume on a region of material containing energy density $\varepsilon(\mathbf{r},t)$. The temporally transient nature of the solution for $\varepsilon(\mathbf{r},t)$ given in eq. 21 means that $-\nabla\varepsilon(\mathbf{r},t)$ is closely related to a sort of 'pressure pulse'. The idea is

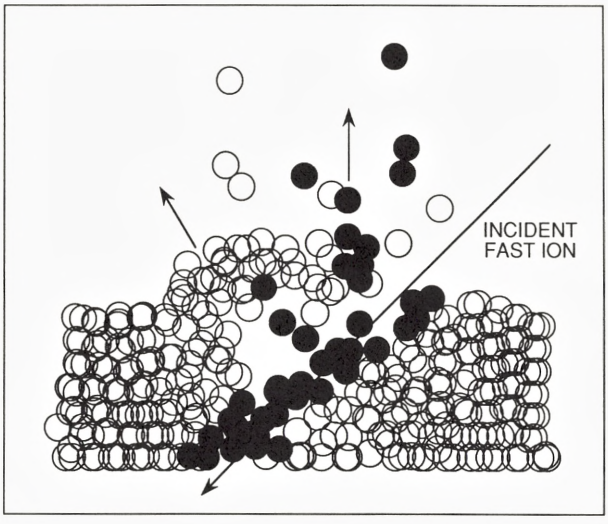

Figure 18. Molecular dynamics simulation of pressure pulse desorption due to depositing potential energy in a cylindrical track by expanding the molecules there. (o) unexpanded molecules; (•) expanded molecules. Expanded molecules are ejected directly in a "popcorn" type effect. Unexpanded molecules eject away from the track direction in response to the correlated volume force. Horizontal scale is roughly 300 Å. Adapted from Fenyö et al. (1990).

applied to the sputtering of organic molecules. The momentum acquired by a molecule experiencing the pressure pulse is:

$$\boldsymbol{p}(\mathbf{r}) = \frac{\beta}{n_{\mathrm{M}}} \int_0^\infty dt[-\boldsymbol{\nabla}\varepsilon(\mathbf{r},t)]. \tag{22}$$

Here, β is a thermodynamical proportionality constant describing the fraction of the energy in the solid which appears as translational kinetic energy rather than as internal energy of molecules. Desorption occurs when a molecule acquires a critical normal momentum which is related to the surface binding energy U:

$$p_\perp \geq p_c = \sqrt{2MU}. \tag{23}$$

The ejection of molecules by a correlated volume force is shown schematically in fig. 16.

The pressure pulse model has been applied to the case of cylindrical ion tracks, which are regarded as a collection of evenly spaced 'mini-pulses' (average spacing λ). The geometry is shown in fig. 17. At depth z, radial distance ρ, and time t,

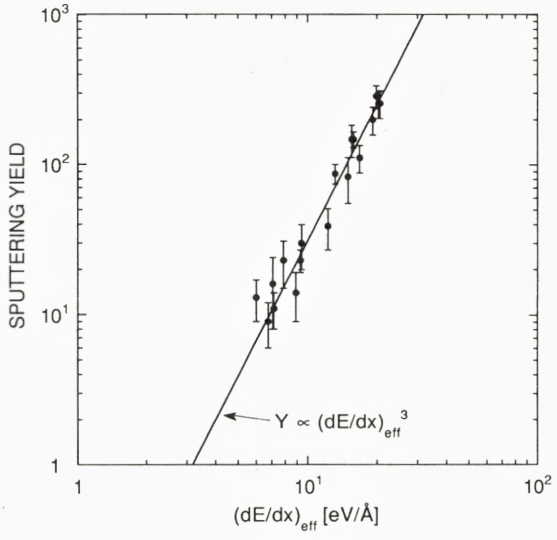

Figure 19. Simulated pressure pulse molecular sputtering yield versus dE/dx. The stopping power scaling is approximately $Y \propto (dE/dx)^3$. Adapted from Fenyö et al. (1990).

the energy density is:

$$\begin{aligned} \varepsilon(\rho, z, t) &= \sum_{i=0}^{\infty} \varepsilon_i(r_i, t) \approx \int_0^{\infty} \varepsilon(\sqrt{\rho^2 + (z' - z)^2}, t) \frac{dz'}{\lambda} \\ &= \frac{\Delta E_{\mathrm{i}}}{\lambda \pi \xi^2(t)} \exp\left(-\frac{\rho}{\xi^2(t)}\right) \frac{1 + \mathrm{erf}[z/\xi(t)]}{2} \end{aligned} \tag{24}$$

where

$$\xi^2(t) = r_0^2 + 4\kappa t \tag{25}$$

The term $(1 + \mathrm{erf}[z/\xi(t)])/2$ decreases in magnitude as z approaches zero, showing that there is an energy gradient at and near the vacuum interface. The surface on which the ejection criterion eq. 23 is satisfied is a half-sphere of radius r_{c}, also shown in fig. 17. The theory does not assert anything on the form in which the material is ejected, but since the gradient is largest at the surface, it may be supposed that molecules are ejected sequentially starting at the surface and then proceeding downwards into the bulk. Identifying the quantity $\Delta E_{\mathrm{i}}/\lambda$ with the stopping power dE/dx, it turns out that r_{c} and the sputtering yield Y scale as follows with dE/dx:

$$r_{\mathrm{c}} \propto \frac{1}{n_{\mathrm{M}}^{2/3} U} \frac{dE}{dx}; \; Y \propto \left(\frac{1}{U} \frac{dE}{dx}\right)^3 . \tag{26}$$

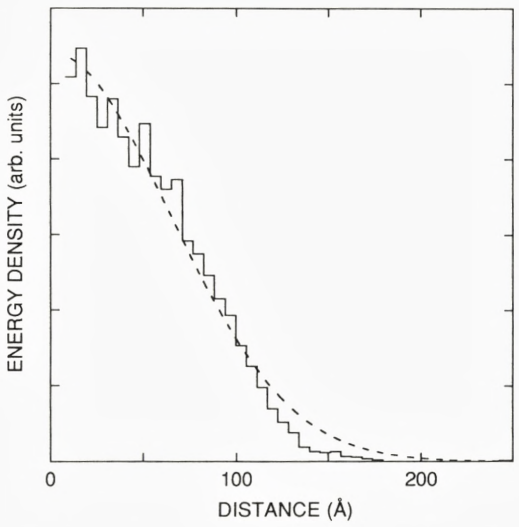

Figure 20. Radial dependence of the energy density from a pressure pulse classical dynamics simulation. The dotted line shows a comparison to the results of the energy diffusion equation. After about 4 psec, the molecular dynamics results and the diffusion equation results are completely consistent. Adapted from Fenyö & Johnson (1992).

For a cylindrical ion track oriented normal to the surface, ejection from the surface is estimated as being about 45° away from the normal direction. If ions are incident at some angle with respect to the surface normal, than the ejection is predicted to be closer to the normal than 45°. In the limit of grazing incidence, then ejection in the plane determined by the ion incidence vector and the surface normal would tend to be along the surface normal.

Fenyö et al. (1990) have performed molecular dynamics simulations of pressure pulse sputtering. Their model solid consisted of a collection of incompressible and structureless 'molecules' of mass 10^4 u which were bound together by a Lennard-Jones potential. An excited 'ion track' was created by depositing potential energy in a narrow cylindrical region of the target. This 'deposition' was performed by 'expanding' the molecules, i.e. by increasing the internuclear separation which yields the minimum potential energy between two neighbouring molecules. As shown in fig. 18, a number of the 'expanded' molecules are directly ejected close to the normal direction. These particles are ejected directly in the 'popcorn' fashion suggested by Williams & Sundqvist (1987). However, a considerable quantity of 'unexpanded' molecules are also ejected in a direction away from the direction of incidence of the impacting ion. These molecules are ejected in response to the

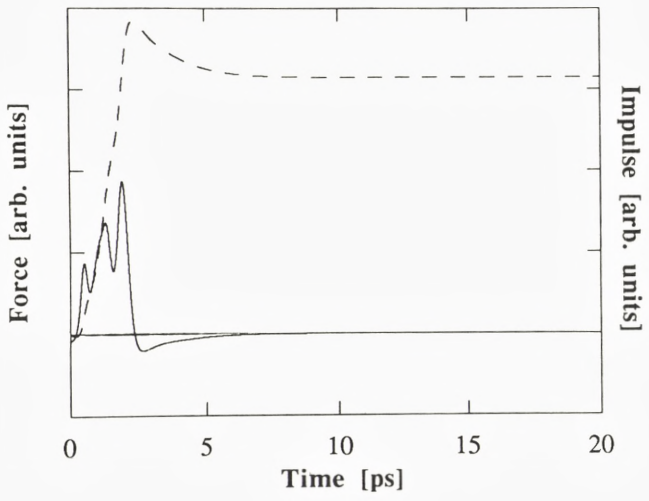

Figure 21. Force (solid line) and impulse (dotted line) experienced by a surface atom as a function of time under the influence of a pressure pulse; from a classical molecular dynamics calculation. In less than 5 psec, the atom in question is desorbed. Adapted from Fenyö & Johnson (1992).

pressure pulse ejection mechanism, as predicted by the analytical pressure pulse model described above. As shown in fig. 19, the yield of desorbed particles per excited track scales very nearly as $Y \propto (dE/dx)_e^3$, again showing consistency with the analytical pressure pulse model.

Fenyö & Johnson (1992) have used the detailed information available in classical dynamics simulations to examine whether a diffusion equation truly describes events occurring in the material surrounding an energized core region created by locally deposited energy. According to their results, the following events occur. First, over 2 to 3 psec, the core potential energy is converted into kinetic energy in the surrounding material. As shown in fig. 20, by 4 psec, the energy density is described diffusively by eq. 24. As shown in fig. 21, some molecules relatively near the center have acquired enough momentum to be desorbed, after a time less than 5 psec, and these are the pressure-pulse desorbed molecules. For times greater than 5 psec, the diffusion equation approach still describes the evolution of energy in the system, but an energy-dependent thermal diffusivity must be taken into account. Johnson et al. (1989) have noted that the conclusions from their analytic pressure pulse model 'will be similar for κ not constant'. As discussed above, the role played by shock waves in the simulation was unclear but appeared to be limited to defining the profile of deposited energy before collisional diffusion sets in. It is interesting that the classical dynamics simulation, although utilizing only detailed

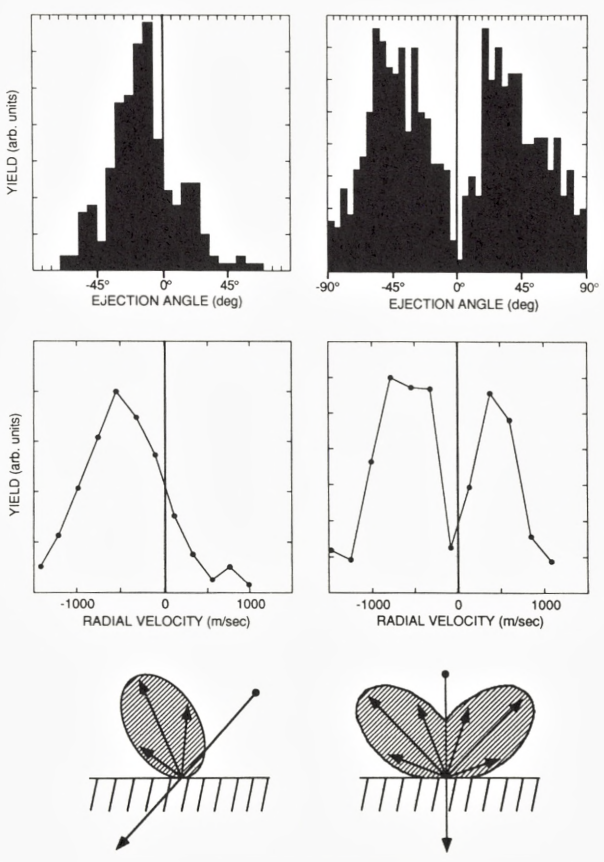

Figure 22. Top: classical molecular dynamics results, ejection angular distributions for off-normal and normal incident ions. Middle: radial velocity distributions for desorbed insulin ions for off-normal and normal incident ions. Bottom: schematic diagram of the sputtered plumes in the two cases. Adapted from Fenyö et al. (1990).

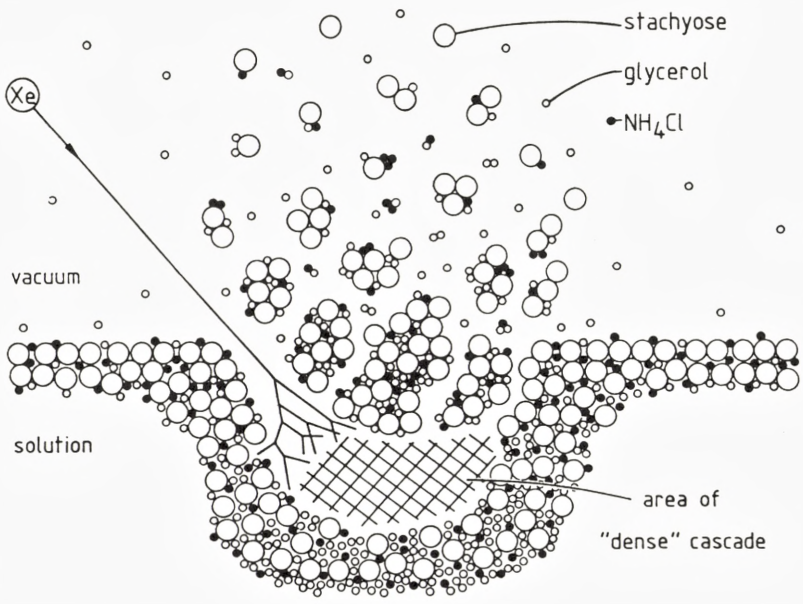

Figure 23. Schematic diagram of pressure pulse desorption due to a keV atomic ion incident on glycerol. Reprinted from Wong & Röllgen (1986) by permission.

'local' or microscopic information on how molecules interact, gives results which are largely consistent with the macroscopic diffusion equation approach which makes no reference whatsoever to the detailed structure of an organic molecular solid.

For the case of MeV atomic ions incident on organic targets, the pressure pulse model quite convincingly accounts for several important observations. For example, the model specifically refers to the dominant neutral molecule ejection yield and predicts a stopping power scaling $Y \propto (dE/dx)_e^3$. This result is consistent with the only known measurement of the neutral desorbed particle yield scaling, performed by Hedin et al. (1987) for the amino acid leucine. The magnitude of the yield, typically of the order of 1000 desorbed molecules per incident ion, is approximately accounted for. Qualitative agreement has also been obtained between the molecular-dynamics-predicted ejection angular distributions and radial velocity distributions obtained by Ens et al. (1989) for desorbed insulin ions. A comparison between these quantities is shown in fig. 22 for two different angles of incidence: 0° (i.e. normal incidence) and 45°. Not surprisingly, the neutrals show a less pronounced off-normal angular ejection pattern but with a similar sense.

Although agreement between the pressure pulse theory and MeV atomic ion

induced desorption results is impressive, caution is still required in assessing the validity of the theory. For example, it is not known experimentally whether the $Y \propto (dE/dx)_e^3$ scaling law holds in general. Also, the angular distributions of desorbed neutral particles have not yet been measured, meaning that only qualitative comparisons may be made between experiment and theoretical predictions. Since the pressure pulse model does not address the complex issue of ionization/neutralization, the different stopping power scaling laws for positive and negative desorbed ion yields remain unexplained. As Ens et al. (1989) and Moshammer et al. (1990) have shown, the angular distributions of ions from various organic samples can differ remarkably from one another in a way that is not clearly accounted for by the pressure pulse model. For example, amino acid monomer ions do not show off-normal ejection under excitation by normally incident ions, although their neutral desorption yield scales as $Y \propto (dE/dx)_e^3$ as predicted by the pressure pulse model. Possibly the ejection of small organic molecules, the only case for which relatively detailed neutral ejection data is available, is best described by thermal models, which can also scale steeply with $(dE/dx)_e$ over a limited range of $(dE/dx)_e$.

Another area in which the pressure pulse concept could be applicable is that of FAB of liquid matrices containing organic analyte molecules. Wong & Röllgen (1986) wrote: 'A concerted momentum transfer to molecules by surrounding atoms or molecules is probably the only mechanism which leaves large, fragile molecules intact in the desorption process'. Their concept for desorption is shown schematically in fig. 23. The authors argue that an incident keV Xe ion penetrates 50 to 100 Å into the matrix, creating a dense cascade and stimulating a vaporization process. A high pressure builds up, ejecting overlying material in the form of clusters of analyte and solvent molecules. During desolvation, vibrationally 'cold' analyte molecules result. Considering remarks made in the introduction and in the section on thermal models concerning the size of the excited region of the target in comparison to the ejected volume, it is considered that the pressure pulse model must be taken seriously as a potential explanation of aspects of keV atom or ion bombardment of liquids.

Yen et al. (1992) have performed an experiment which can be interpreted as corroborating the pressure pulse idea for keV atomic ion bombardment of glycerol matrices. They deployed a charged HDPA surfactant on the surface of glycerol to define a layer of a preformed ionic analyte, dAMP, just below the surface. keV Ga^+, In^+, Bi^+, as well as ionic dimers and trimers of Bi and Au, were used to bombard this system, and the ion yield of dAMP was observed to scale as follows with the nuclear stopping cross section S_n: $Y \propto (S_n - \text{thresh})^2$. Assuming that the detected species may only come from the surface of the glycerol-surfactant system, the desorption geometry is strictly two dimensional. Referring to eq. 26, it can be

seen that the pressure pulse model would predict approximately square-law stopping power scaling ($Y \propto r_c^2 \propto S_n^2$), in qualitative agreement with the experimental observation. (By analogy with the simulation result of Whitlow et al. (1987), the excitation geometry may be considered to be approximately cylindrical.) Standing et al. (1982) have measured the primary ion energy dependence of alkali ion induced sputtering of ions from solid alanine. Ens (1992) has shown that, particularly for the heavier alkali ions, the ion yield is well described by the relation $Y \propto S_n^3$. If it may be assumed that ions are emitted from the bulk as well as the surface for the case of the solid analine, then this result is also qualitatively consistent with the pressure pulse model. Ens et al. (1989) also measured radial velocity distributions for insulin ions desorbed by keV Cs^+ and MeV ^{252}Cf fission fragments. Secondary ion mass spectra were surprisingly similar, but Cs^+ bombardment did not produce pronounced off-normal ejection, as might have been expected if there is pressure pulse desorption such as is considered to occur for MeV ^{252}Cf fission fragment excitation. Perhaps the excitation geometries are not sufficiently alike, or perhaps insulin and analine targets give different results for other reasons. More work is needed to ascertain whether the pressure pulse concept may be applied to keV ion induced sputtering of organics, but there is clearly some promise that it does.

7 Concluding Remarks

In this review, a number of theoretical desorption models have been discussed and evaluated as to their ability to describe energetic particle beam induced desorption of large, thermally labile bio-organic molecules. The following models were discussed: collision cascade; ion track; evaporative thermal spike; bulk desorption; shock wave; and pressure pulse. Although the models as expressed have a degree of generality, they each tend to refer only to a part of the overall process that starts with projectile impact and ends with the detection of an ionic or neutral desorbed particle. Also, experimental situations considered were quite varied, including both solid and liquid organic targets and bombardment by keV and MeV atomic and cluster ions. Given the wide range of situations that it is desirable to model and the limited scope of each theory, it is not surprising that no one model can be found that describes everything. In some cases, it is quite plausible that two or more models apply simultaneously. For example, in the case of keV atomic ion bombardment of liquid organic matrices commonly employed in FAB mass spectroscopy, evidence of collision cascade sputtering can be seen along with the dominant bulk desorption mechanism. As another example, the precise role of shock waves in causing desorption is rather uncertain. The role of a shock wave could be merely to heat a region of a target, after which bulk desorption may occur.

In the case of cluster ion bombardment of organic targets, the operative desorption mechanism is unknown, but evaporative thermal spike, bulk desorption, pressure pulse, and shock wave mechanisms have all been convincingly invoked to rationalize the observations.

The desorption of a large bio-organic molecule without significant fragmentation requires a considerable impulse without significant accompanying internal energy. 'Volume forces' and 'collective' motion of the lattice can satisfy these requirements and lead to desorption of intact molecules relatively far from the area of initial excitation. Consequently, the bulk desorption, shock wave, and pressure pulse models are most appealing as candidates for describing large molecule desorption. Possibly the pressure pulse model may be considered to be the most general model that has been proposed so far. This model is roughly consistent with much of the body of data on MeV-atomic-ion-induced desorption of organic molecules and can be employed to rationalize many features of keV atomic- and cluster-ion bombardment of organic targets as well. Molecular dynamics simulations, based on a purely microscopic interaction picture, give results consistent with the analytical pressure pulse model and its macroscopic viewpoint of assumed diffusion of energy density with no reference to detailed structure and interactions. This impressive agreement is a further indication that ejection of whole molecules by an energy gradient volume force is a feasible desorption mechanism.

Although bulk desorption and the pressure pulse/shock wave models are most able to explain the desorption of large molecules under particle impact, there are cases for which the other models considered, such as the collision cascade, ion track, and evaporative thermal spike models, have some validity. For example, evaporative models may provide an adequate explanation for MeV ion-induced desorption of small organic molecules, and the collision cascade model describes the high kinetic energy component of molecules desorbed from liquid matrices under keV atomic ion bombardment.

Several directives for future work should be considered. For example, nearly every theory makes predictions concerning sputtered neutral molecules, whereas nearly every experiment is based on the detection and analysis of sputtered ions. This discrepancy is a serious one that hinders comparisons between data and theory. It is therefore recommended that theorists perform more detailed analyses of ionization and neutralization processes, and that experimentalists make serious efforts to measure neutral molecule yields and kinetic energy- and angle-resolved ejection distributions. Atomic force microscopy imaging of ion impact 'craters' and multiphoton ionization probes of neutral ejecta would be two effective means of extending our knowledge on the behavior of neutral desorbed molecules. Also, it is noted that well-designed computer 'gedanken experiments' provide powerful insight into the response of matter to energetic particle excitation. As has been

convincingly demonstrated by a number of workers, molecular dynamics is a powerful tool for investigating the link between microscopic interactions and macroscopic behavior. However, current simulations of ion impacts on organic targets regard the target molecules as point particles, and it would be a significant advance if the internal structure of the molecular target particles could be also taken into account. This would lead to a better analysis of conditions under which varying amounts of internal excitation of desorbed molecules occurs, a subject which has not yet been thoroughly investigated.

The overall conclusion of this account is that some very impressive models of bio-organic molecule ejection have been generated. The pressure pulse model of ejection seems to be the most generally applicable model available at this time, but one must be aware of certain subsets of the observations that may require invoking other desorption models in order to be adequately explained. With appropriate extensions of existing experimental, theoretical, and calculational art, the prospects for attaining a thorough understanding of macromolecular desorption are quite promising.

Acknowledgments

The author expresses his gratitude towards a number of individuals for their help in understanding the theoretical models and experimental background discussed herein, including Jörgen Ahlbom, Iosif Bitensky, Plamen Demirev, Jan Eriksson, David Fenyö, Per Håkansson, and Robert E. Johnson. He also thanks Bo U.R. Sundqvist for many useful discussions and for the opportunity to be a part of the Ion Physics Group at Uppsala where much work in the field of ion-induced desorption of biomolecules is carried out. He is also appreciative of P. Sigmund for the opportunity to participate in the SPUT92 conference. Finally, the author is grateful for the financial support provided by the Swedish Research Council for Engineering Sciences.

References

Balaji V, David DE, Magnera TF, Michl J and Urbassek HM, 1990: Nucl. Instrum. Meth. B **46**, 435

Barber M, Bordoli RS, Sedgewick RD and Taylor AN, 1981: J. Chem. Soc., Chem. Commun., 325

Barofsky DF and Barofsky E, 1986: *Ion Formation from Organic Solids (IFOS III)*, ed. Benninghoven A, Springer-Verlag, Berlin, 86

Barofsky DF, Ilias AM, Barofsky E and Murphy JH, 1984: *32nd Ann. Conf. Mass Spectrom. and Allied Topics*, San Antonio, Book of Abstracts, 186

Barofsky DF, Jiang L-F, Barofsky E and Yen T-Y, 1991: *Methods and Mechanisms for Producing Ions from Large Molecules*, eds. Standing KG and Ens W, Plenum Press, New York, 101

Benninghoven A, Jaspers D and Sichtermann W, 1976: Appl. Phys. **11**, 35
Bitensky IS and Parilis ES, 1987: Nucl. Instrum. Meth. B **21**, 26
Bitensky IS, Goldenberg AM and Parilis ES, 1989: J. de Physique C **2**, 213
Bitensky IS, Goldenberg AM and Parilis ES, 1990: *Ion Formation from Organic Solids (IFOS V)*, eds. Hedin A et al., John Wiley and Sons, New York, 205
Bitensky IS, Goldenberg AM and Parilis ES, 1991: *Methods and Mechanisms for Producing Ions from Large Molecules*, eds. Standing KG and Ens W, Plenum Press, New York, 83
Brandt W and Ritchie RH, 1974: *Physical Mechanisms in Radiation Biology*, eds. Cooper RD and Wood RD, USEC Technical Inf. Center, Oak Ridge, Tennessee, 20
Carter G, 1983: Nucl. Instrum. Meth. **209/210**, 1
David DE, Magnera TF, Tian R, Stulik D and Michl J, 1986: Nucl. Instrum. Meth. B **14**, 378
Demirev PA, 1988: Adv. in Mass Spect. **11A**, 460
Ens W, 1992: Mat. Fys. Medd. Dan. Vid. Selsk. **43**, 155
Ens W, Sundqvist BUR, Håkansson P, Hedin A and Jonsson G, 1989: Phys. Rev. B **39**, 763
Ens W, Sundqvist BUR, Håkansson P, Fenyö D, Hedin A and Jonsson G, 1989a: J. de Physique C **2**, 9
Falcone G, 1987: Surf. Sci. **187**, 212
Falcone G, 1990: La Rivista del Nuovo Cimento, 1
Falcone G, Sroubek Z, Sindona G and Uccella N, 1988: Int. J. of Mass Spect. and Ion Phys. **83**, 223
Fenyö D and Johnson RE, 1992: Phys. Rev. B **46**, 5090
Fenyö D, Sundqvist BUR, Karlsson BR and Johnson RE, 1990: Phys. Rev. B **42**, 1895
Fenyö D, Hedin A, Håkansson P and Sundqvist BUR, 1990a: Int. J. of Mass Spectrom. and Ion Proc. **100**, 63
Garrison BJ, 1983: Int. J. of Mass Spect. and Ion Phys. **53**, 243
Gol'danskii VI, Lantsburg EYa and Yampol'skii PA, 1975: JETP Lett. **21**, 166
Haring RA, Roosendaal HE and Zalm PC, 1987: Nucl. Instrum. and Meth. B **28**, 205
Hedin A, Håkansson P, Sundqvist BUR and Johnson RE, 1985: Phys. Rev. B **31**, 1780
Hedin A, Håkansson P, Salehpour M and Sundqvist BUR, 1987: Phys. Rev. B **35**, 7377
Holian BL, Hoover WG, Moran B and Straub GK, 1980: Phys. Rev. A **22**, 2798
Hoogerbrugge R and Kistemaker PG, 1987: Nucl. Instrum. Methods B **21**, 37
Hoogerbrugge R, Van der Zande WJ and Kistemaker PG, 1987: Int. J. of Mass Spect. and Ion Proc. **76**, 239
Hoogerbrugge R, Bobeldijk M, Kistemaker PG and Los J, 1988: J. Chem. Phys. **88**, 5314
Johnson RE, 1987: Int. J. of Mass Spectrom. and Ion Proc. **78**, 357
Johnson RE, 1990: *Energetic Charged-Particle Interactions with Atmospheres and Surfaces*, Springer-Verlag, Berlin
Johnson RE and Evatt R, 1980: Rad. Eff. **52**, 187
Johnson RE and Sundqvist BUR, 1992: Physics Today, March, 28
Johnson RE, Sundqvist BUR, Hedin A and Fenyö D, 1989: Phys. Rev. B **40**, 49
Johnson RE, Pospieszalska M and Brown WL, 1991: Phys. Rev. B **44**, 7263
Junack M, Sichtermann W and Benninghoven A, 1986: *Ion Formation from Organic Solids (IFOS III)*, ed. Benninghoven A, Springer-Verlag, Berlin, 96
Karas M and Hillenkamp F, 1988: Anal. Chem. **60**, 2299
Katz R, 1968: Nuclear Track Detection **2**, 1
Kaufmann R, Kirsch D, Rood H-A and Spengler B, 1992: Rap. Comm. in Mass Spect. **6**, 98
Kelly R, 1990: Nucl. Instrum. Meth. B **46**, 441
Kelner L and Markey SP, 1984: Int. J. of Mass Spect. and Ion Proc. **59**, 157
Kitazoe Y, Hiraoka N and Yamamura Y, 1981: Surf. Sci. **111**, 381
Können GP, Tip A and de Vries AE, 1975: Rad. Eff. **26**, 23

Landau LD and Lifschitz EM, 1959: *Fluid Mechanics*, Reading, Massachussetts
Ledbetter MC, Beuhler RJ and Friedman L, 1987: Proc. Natl. Acad. Sci. USA **84**, 85
Lee S-L and Lucchese RA, 1989: J. de Physique C **2**, 231
Lucchese RR, 1987: J. Chem. Phys. **86**, 443
Macfarlane RD, 1982: Acc. Chem. Res. **15**, 268
Macfarlane RD, 1982a: Nucl. Instrum. and Methods **198**, 75
Macfarlane RD and Torgerson DF, 1976: Science **191**, 920
Macfarlane RD and Torgerson DF, 1976a: Phys. Rev. Lett. **36**, 486
Mahoney JF, Perel J, Ruatta SA, Martino PA, Husain S and Lee TD, 1991: Rap. Comm. in Mass Spect. **5**, 441
Mahoney JF, Perel J, Lee TD, Martino PA and Williams P, 1992: J. Am. Soc. Mass Spectrom. **3**, 311
Martens J, Ens W, Standing KG and Verentchikov A, 1992: Rap. Comm. in Mass Spect. **6**, 147
Matthew MW, Beuhler RJ, Ledbetter M and Friedman L, 1986: Nucl. Instrum. Meth. B **14**, 448
Moshammer R, 1991: Thesis, Institut für Kernphysik, Techn. Hochschule Darmstadt, Germany
Moshammer R, Matthäus R, Wien K and Bolbach G, 1990: *Ion Formation from Organic Solids (IFOS V)*, eds. Hedin A et al., John Wiley and Sons, New York, 17
Mozumder A, 1969: Adv. Radiat. Chem. **1**, 1
Ollerhead RW, Bøttiger J, Davies JA, L'Ecuyer J, Haugen HK and Matsunami N, 1980: Rad. Eff. **49**, 203
Parilis ES, Kishinevsky LM, Turaev NYu, Baklitzky BE, Umarov FF, Verleger VKh, Nizhnaya SL and Bitensky IS, 1993: *Atomic Collisions on Solid Surfaces*, Elsevier Science Publishers, Amsterdam, 339
dePauw E, 1986: Mass Spectrosc. Rev. **5**, 191
Robertson DH, Brenner DW and White CT, 1991: Phys. Rev. Lett. **67**, 3132
Salehpour M, Håkansson P, Sundqvist BUR and Widdiyasekera S, 1986: Nucl. Inst. Meth. B **13**, 278
Seiberling LE, Griffith JE and Tombrello TA, 1980: Rad. Eff. **52**, 201
Shapiro MH and Tombrello TA, 1992: Unpublished presentation at *SPUT92*
Shiea JT and Sunner J, 1990: Int. J. of Mass Spect. and Ion Proc. **96**, 243
Shiea JT and Sunner J, 1991: *Methods and Mechanisms for Producing Ions from Large Molecules*, eds. Standing KG and Ens W, Plenum Press, New York, 147
Sigmund P, 1969: Phys. Rev. **184**, 383
Sigmund P, 1969a: Phys. Rev. **187**, 768
Sigmund P, 1974: Appl. Phys. Lett. **25**, 169
Sigmund P, 1981: *Sputtering by Ion Bombardment, Vol. I*, ed. by Berisch R, Springer, Berlin, 8
Sigmund P, 1989: J. de Physique C **2**, 175
Sigmund P and Claussen C, 1981: J. Appl. Phys. **52**, 990
Standing KG, Chait BT, Ens W, McIntosh G and Beavis R, 1982: Nucl. Instrum. and Methods B **198**, 33
Sundqvist BUR, 1991: *Sputtering by Particle Bombardment Vol. III*, eds. Behrisch R and Wittmaack K, Springer-Verlag, Berlin, 257
Sunner J, 1990: *Ion Formation from Organic Solids (IFOS V)*, eds. Hedin A et al., A, John Wiley and Sons, New York, 175
Sunner J, Morales A and Kebarle P, 1988: Int. J. of Mass Spect. and Ion Proc. **86** 169
Sunner J, Ikonomou MG and Kebarle P, 1988a: Int. J. of Mass Spect. and Ion Proc. **82**, 221
Torgerson DF, Skowronski RP and Macfarlane RD, 1974: Biochem. Biophys. Res. Commun. **60**, 616
Urbassek HM, 1987: Nucl. Instrum. Meth. B **18**, 587

Urbassek HM and Michl J, 1987: Nucl. Instrum. Meth. B **22**, 480
Urbassek HM and Sigmund P, 1984: Appl. Phys. A **35**, 19
Urbassek HM and Waldeer KT, 1991: Phys. Rev. Lett. **67**, 105
Vineyard GH, 1976: Rad. Eff. **29**, 245
Wagner NJ, Holian BL and Voter AF, 1992: Phys. Rev. A **45**, 8457
Waldeer KT and Urbassek HM, 1993: Nucl. Instrum. Meth. B **73**, 14
Whitlow HJ, Hautala M and Sundqvist BUR, 1987: Int. J. of Mass Spectrom. and Ion Proc. **78**, 329
Williams P and Sundqvist BUR, 1987: Phys. Rev. Lett. **58**, 1031
Wong SS and Röllgen FW, 1986: Nucl. Instrum. Meth. B **14**, 436
Wong SS, Röllgen FW, Manz I and Przybylski M, 1985: Biomed. Mass Spectrom. **12**, 43
Yen TY, 1992: Thesis, Dept. of Agricultural Chemistry, Oregon State University
Yen TY, Barofsky E and Barofsky DF, 1992: Poster presented at SPUT92, Copenhagen
Zel'dovich YaB and Raizer YuP, 1967: *Physics of Shock Waves and High-Temperature Hydrodynamic Phenomena*, eds. Hayes WD and Probstein RF, Academic Press, New York
Zel'dovich Ya and Todes OM, 1940: Zh. Eksp. Fiz. **10** 1441